

# Kernel regression in high dimension: Refined analysis beyond double descent

Fanghui Liu\*   Zhenyu Liao<sup>†</sup>   Johan A.K. Suykens\*

June 4, 2022

## Abstract

In this paper, we provide a precise characterization of generalization properties of high dimensional kernel ridge regression across the under- and over-parameterized regimes, depending on whether the number of training data  $n$  exceeds the feature dimension  $d$ . By establishing a novel bias-variance decomposition of the expected excess risk, we show that, while the bias is independent of  $d$  and monotonically decreases with  $n$ , the variance depends on  $n, d$  and can be unimodal or monotonically decreasing under different regularization schemes. Our refined analysis goes beyond the double descent theory by showing that, depending on the data eigen-profile and the level of regularization, the kernel regression risk curve can be a double-descent-like, bell-shaped, or monotonic function of  $n$ . Experiments on synthetic and real data are conducted to support our theoretical findings.

## 1 Introduction

Interpolation learning [MM19, HMRT19, BLLT20] has recently attracted growing attention in the machine learning community. This is mainly because current state-of-the-art neural networks appear to be models of this type, that are able to interpolate training data while still generalizing well on test data, even in the presence of label noise [ZBH<sup>+</sup>16]. It has been empirically observed that other models including kernel methods, decision trees, and as simple as linear regression also exhibit similar phenomenon [BLLT20, BHMM19]. This is somewhat striking as it goes against the conventional wisdom of *bias-variance trade-off* [CS02]: predictors that generalize well should trade off the model complexity and fitting on training data. The double descent explanation [BHMM19] resolves this paradox by revisiting the bias-variance trade-off and showing that, the generalization error of learning models exhibits a phase transition at the *interpolation threshold*: moving away from this threshold on both sides trends to reduce the generalization error.

The double descent phenomenon has recently inspired intense theoretical researches. One line of work formalized the argument that, even when no explicit regularization is imposed, *implicit regularization* is encoded in the model via the choice of optimization algorithms and techniques, e.g., stochastic gradient descent (SGD) [HRS16], dropout [SHK<sup>+</sup>14], early stopping [AKT19], and ensemble methods [LJB20]. Different from the above external schemes, kernel interpolation estimator [LR20, BRT19] directly benefits from its intrinsic kernel structure, that serves as an *implicit regularization* to help both interpolate and approximate. In fact, (strictly) positive-definite kernels can interpolate an arbitrary number of data points [Wen04], and thus kernel spaces contain (nearly) optimal interpolants [GMMM19, Li20]. Although the kernel space is rich enough to contain models that generalize well, the generalization property of a specific choice of kernel, and in particular, its interplay with the data and the level of regularization, still remains unclear, especially in the over-parameterized regime. An telling example, whether (or not) the double descent phenomenon exists in the kernel regression model is still an open question [LR20, BCP20]. As such, novel and refined analyses are needed to have a thorough understanding of kernel estimators, in the high dimensional regime of interest. This is indeed the ultimate objective of the article.

\*Department of Electrical Engineering (ESAT-STADIUS), KU Leuven

<sup>†</sup>Department of Statistics, University of California, Berkeley

**Table 1.** The trends of the variance  $\mathbf{V}$  with respect to  $n$  in the  $n < d$  case. The notation  $\nearrow$  means the variance  $\mathbf{V}$  increases with  $n$ ;  $\rightarrow$  indicates that  $\mathbf{V}$  stays unchanged;  $\searrow$  means  $\mathbf{V}$  decreases with  $n$ , see Figure 1(a); and  $r_* := \text{rank}(\mathbf{X}\mathbf{X}^\top/d)$ . From the left column to the right column, the regularization parameter  $\lambda$  increases, and a large  $\lambda$  leads to a small value of the peak point  $n_* := n_*(\lambda)$ , and even the peak will disappear. Note that the value  $n_*$  is different in three eigenvalue decays of  $\mathbf{X}\mathbf{X}^\top/d$ . Refer to Section 4.1 for details.

eigenvalue decay	$\lambda = 0$	$\lambda := \bar{c}n^{-\vartheta}$ (KRR)				
harmonic decay	$\nearrow \rightarrow$	$1 \geq \vartheta \geq \frac{1}{2(2-\bar{c})}$	$\vartheta < \frac{1}{2(2-\bar{c})}$			
		$\nearrow \rightarrow$	$r_* < d \leq n_*$	$r_* \leq n_* \leq d$	$n_* \leq r_* < d$	$n_* \leq c < r_* < d$ <sup>1</sup>
polynomial decay	$\nearrow \rightarrow$	$1 \geq \vartheta \geq \frac{1}{1+\frac{1}{2a}}$	$\vartheta < \frac{1}{1+\frac{1}{2a}}$			
		$\nearrow \rightarrow$	$r_* < d \leq n_*$	$r_* \leq n_* \leq d$	$n_* \leq r_* < d$	$n_* \leq c < r_* < d$
exponential decay	$\nearrow \rightarrow$		$r_* < d \leq n_*$	$r_* \leq n_* \leq d$	$n_* \leq r_* < d$	$n_* \leq c < r_* < d$

<sup>1</sup> Here  $c$  is some constant such that  $n > c$  always holds as  $n$  is required to be large in theory and practice.

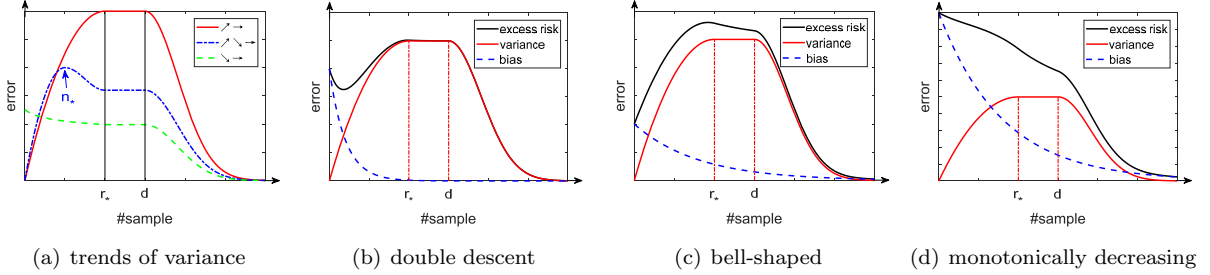


**Figure 1.** (a) Trends of variance under different regularization schemes corresponding to Table 1. (b-d) Trends of the risk curve under various bias and variance can be double descent, bell-shaped, and monotonically decreasing.

Here, we consider the kernel ridge regression (KRR) estimator [CS02, SSM97, SVGDB<sup>+</sup>02] in a high dimensional setting, and treat the kernel interpolation as the limit of KRR by taking the explicit regularization to be zero. More precisely, by virtue of the linearization of kernel matrices in high dimension [LR20, EK10, EKZ<sup>+</sup>20], we disentangle the implicit regularization of kernel interpolation estimators in an explicit manner. As a result, both implicit and explicit regularization schemes can be systematically studied under our framework. Mathematically, KRR aims to solve the following empirical risk minimization problem on a given training set  $\mathbf{z} := \{(\mathbf{x}_i, y_i)\}_{i=1}^n$  with data  $\mathbf{x}_i \in \mathbb{R}^d$  and responses  $y_i \in \mathbb{R}$ :

$$f_{\mathbf{z}, \lambda} := \operatorname{argmin}_{f \in \mathcal{H}} \left\{ \frac{1}{n} \sum_{i=1}^n (f(\mathbf{x}_i) - y_i)^2 + \lambda \langle f, f \rangle_{\mathcal{H}} \right\}, \quad (1.1)$$

where an explicit Tikhonov regularization term induced by a reproducing kernel Hilbert space (RKHS)  $\mathcal{H}$  is added to the least-squares objective. In statistical learning theory [CZ07], the regularization parameter  $\lambda > 0$  is generally taken to depend on the sample size  $n$  in such a way that  $\lim_{n \rightarrow \infty} \lambda(n) = 0$ . Here we mathematically assume that  $\lambda := \bar{c}n^{-\vartheta}$  with some  $\vartheta \geq 0$  and  $0 \leq \bar{c} \leq 1$  so as to cover the interpolation case. In this paper, we propose a novel bias-variance decomposition of the KRR expected excess risk, and derive non-asymptotic bounds for both bias and variance. This precise assessment leads to fruitful discussions as a function of different data eigenvalue decays and regularization schemes. Our main findings include:

- We demonstrate that, for a large data dimension  $d$ , the kernel matrix admits the same eigenvalue decay as  $\mathbf{X}\mathbf{X}^\top/d$ , where  $\mathbf{X} = [\mathbf{x}_1, \mathbf{x}_2, \dots, \mathbf{x}_n]^\top \in \mathbb{R}^{n \times d}$  is the data matrix. So in high dimension, the eigenvalue decay of  $\mathbf{K}$  is almost determined by the data itself, which will be reflected in our error bound for the bias.

- The explicit regularization  $\lambda := \bar{c}n^{-\vartheta}$  largely affects the peak point of the variance: a large  $\lambda$  decreases the model complexity, and thus the interpolation threshold  $n_* \equiv n_*(\lambda)$  moves to a small value. Table 1 shows that, under a small (or zero) regularization so that  $r_* \leq n_*$  with  $r_* := \text{rank}(\mathbf{X}\mathbf{X}^\top/d)$ : the variance monotonically increases with  $n$  until  $n := r_*$ , as in the red curve of Figure 1(a). Under a moderate regularization with  $n_* \leq r_*$ :  $V$  first increases with  $n$  until  $n := n_*$  and then decreases. In this case, the peak point will be in advance due to  $n_* < d$ , see the blue curve in Figure 1(a). Under a large regularization such that  $n_* \leq c$ , where  $c$  is some constant, the variance monotonically decreases of  $n$ , see the green curve in Figure 1(a). Note in particular that, taking  $\lambda$  independent of  $n$ ,  $\lambda$  only effects the magnitude (instead of the position) of the peak point. This is consistent with the results in [HMRT19].
- Our error bounds for the bias and the variance exhibit different characteristics. More specifically, the error bound for the bias is independent of the data/feature dimension  $d$ . It monotonically decreases with  $n$  at a certain  $\mathcal{O}(\lambda)$  learning rate as in the classical learning theory [CZ07, WZ11, SS07]. Nevertheless, the variance curve depends on  $n$  and  $d$ , and exhibits monotonic decreasing or unimodal with  $n$  under different regularizations. Hence, the expected excess risk, as the sum of bias and variance, can be double descent (Figure 1(b)), bell-shaped (Figure 1(c)), and monotonic decreasing (Figure 1(d)), depending on the level of *implicit* or *explicit* regularization. This phenomenon is in agreement with empirical findings in neural networks [YYY+20] and we theoretically answer their question in kernel regression: why the variance is unimodal and the bias is monotonically decreasing.
- Our results show that, for fixed  $d$ , both the variance and bias tends to zero as  $n \rightarrow \infty$  under the  $\lambda := \bar{c}n^{-\vartheta}$  regularization scheme, which implies that the excess risk approaches to zero. Based on this, in the double descent case particularly, the minimum of the expected error in the over-parameterized  $n > d$  regime is lower than that in the  $n < d$  regime. This claim cannot be obtained from [LR20] where the expected risk is only shown to converge to a constant.

The rest of the paper is organized as follows. We briefly introduce problem settings in Section 2. In Section 3, we present our main results on the generalization property of KRR in high dimension and briefly sketch the main ideas of the proof. Discussions on the derived error bounds are given in Section 4. In Section 5, we report numerical experiments to support our theoretical results and the conclusion is drawn in Section 6.

## 2 Problem Settings and Preliminaries

We work in the high dimensional regime for some large  $d, n$  with  $c \leq d/n \leq C$  for some constants  $c, C > 0$ . For notational simplicity, we denote by  $a(n) \lesssim b(n)$ : there exists a constant  $\tilde{C}$  independent of  $n$  such that  $a(n) \leq \tilde{C}b(n)$ , and analogously for  $\asymp$  and  $\gtrsim$ .

### 2.1 Kernel Ridge Regression Estimator

Let  $X \subseteq \mathbb{R}^d$  be a metric space and  $Y \subseteq \mathbb{R}$ , the instances  $(\mathbf{x}_i, y_i)$  in the training set  $\mathbf{z} = \{(\mathbf{x}_i, y_i)\}_{i=1}^n \in Z^n$  are assumed to be independently drawn from a non-degenerate Borel probability measure  $\rho$  on  $X \times Y$ . The *target function* of  $\rho$  is defined by

$$f_\rho(\mathbf{x}) = \int_Y y d\rho(y | \mathbf{x}), \quad \mathbf{x} \in X, \quad (2.1)$$

where  $\rho(\cdot | \mathbf{x})$  is the conditional distribution of  $\rho$  at  $\mathbf{x} \in X$ . Define the response vector  $\mathbf{y} = [y_1, y_2, \dots, y_n]^\top \in \mathbb{R}^n$  and the kernel matrix  $\mathbf{K} = \{k(\mathbf{x}_i, \mathbf{x}_j)\}_{i,j=1}^n$  induced by a positive definite kernel  $k(\cdot, \cdot)$ , KRR aims to find a hypothesis  $f : X \rightarrow Y$  such that  $f(\mathbf{x})$  is a good approximation of the response  $y \in Y$  corresponding to a new instance  $\mathbf{x} \in X$ . This is actually an empirical risk minimization in problem (1.1). By denoting  $k(\mathbf{x}, \mathbf{X}) = [k(\mathbf{x}, \mathbf{x}_1), k(\mathbf{x}, \mathbf{x}_2), \dots, k(\mathbf{x}, \mathbf{x}_n)]^\top \in \mathbb{R}^n$ , the closed-form of KRR estimator in Eq. (1.1) is

$$f_{\mathbf{z}, \lambda}(\mathbf{x}) = k(\mathbf{x}, \mathbf{X})^\top (\mathbf{K} + n\lambda \mathbf{I})^{-1} \mathbf{y}. \quad (2.2)$$

We consider two popular positive definite kernel classes of (i) the inner-product kernel of the form  $k(\mathbf{x}_i, \mathbf{x}_j) = h(\langle \mathbf{x}_i, \mathbf{x}_j \rangle / d)$  and (ii) the *radial* kernel function  $k(\mathbf{x}_i, \mathbf{x}_j) = h(\|\mathbf{x}_i - \mathbf{x}_j\|_2^2 / d)$ . Here  $h(\cdot) : \mathbb{R} \rightarrow \mathbb{R}$  is a

nonlinear function that is assumed to be (locally) smooth, as in [EK10, LR20]. Examples include commonly used kernels such as linear kernels, polynomial kernels, Sigmoid kernels, exponential kernels, and Gaussian kernels, to name a few.

The expected (quadratic) risk is defined as  $\mathcal{E}(f) = \int_Z (f(\mathbf{x}) - y)^2 d\rho$  and the empirical risk functional is defined on the training set  $\mathbf{z}$ , i.e.,  $\mathcal{E}_{\mathbf{z}}(f) = \frac{1}{n} \sum_{i=1}^n (f(\mathbf{x}_i) - y_i)^2$ . To measure the estimation quality of  $f_{\mathbf{z},\lambda}$ , one natural way is the *expected excess risk*:  $\mathbb{E}_{y|\mathbf{x}}[\mathcal{E}(f_{\mathbf{z},\lambda}) - \mathcal{E}(f_{\rho})]$ . Specifically, in KRR, the expected excess risk admits  $\mathbb{E}_{y|\mathbf{x}}[\mathcal{E}(f_{\mathbf{z},\lambda}) - \mathcal{E}(f_{\rho})] = \mathbb{E}_{y|\mathbf{x}}\|f_{\mathbf{z},\lambda} - f_{\rho}\|_{\mathcal{L}_{\rho_X}^2}^2$ , which is exactly in the weighted  $\mathcal{L}^2$ -space with the norm  $\|f\|_{\mathcal{L}_{\rho_X}^2}^2 = \int_X |f(\mathbf{x})|^2 d\rho_X(\mathbf{x})$ .

## 2.2 Background on RKHS

Now we characterize the integral operators defined by a kernel. Given a kernel  $k$ , its integral operator  $L_K : \mathcal{L}_{\rho_X}^2 \rightarrow \mathcal{L}_{\rho_X}^2$  admits

$$(L_K f)(\cdot) = \int_X k(\cdot, \mathbf{x}) f(\mathbf{x}) d\rho_X(\mathbf{x}), \quad \forall f \in \mathcal{L}_{\rho_X}^2. \quad (2.3)$$

Since  $L_K$  is compact, positive definite and self-adjoint, by the spectral theorem (see, Theorem A.5.13 in [SA08]), there exists countable pairs of eigenvalues and eigenfunctions  $\{\mu_i, \psi_i\}_{i=1}^{\infty}$  of  $L_K$  such that  $L_K \psi_i = \mu_i \psi_i$ , where  $\{\psi_i\}_{i=1}^{\infty}$  are orthogonal basis of  $\mathcal{L}_{\rho_X}^2(X)$  and  $\mu_1 \geq \mu_2 \geq \dots > 0$  with  $\lim_{i \rightarrow \infty} \mu_i = 0$ . Accordingly, by Mercer's theorem, we have  $k(\mathbf{x}, \mathbf{x}') = \sum_{i=1}^{\infty} \mu_i \psi_i(\mathbf{x}) \psi_i(\mathbf{x}')$ , and there exists a constant  $\kappa \geq 1$  such that  $\sup_{\mathbf{x} \in X} \sum_{i=1}^{\infty} \mu_i \psi_i^2(\mathbf{x}) \leq \kappa^2$ . It holds by  $\kappa := \max\{1, \sup_{\mathbf{x} \in X} \sqrt{k(\mathbf{x}, \mathbf{x})}\}$ . Based on the data matrix  $\mathbf{X}$  and the integral operator  $L_K$ , the empirical integral operator is given by  $L_{K, \mathbf{X}} = \frac{1}{n} \sum_{i=1}^n k(\cdot, \mathbf{x}_i) \otimes k(\cdot, \mathbf{x}_i)$ , which converges to the data-free limit  $L_K$  at an  $\mathcal{O}(1/\sqrt{n})$  rate [DMDVR09].

## 3 Main Results

In this section, we state our main result under some basic/technical assumptions, compare it with existing results, and sketch the main ideas of our proof.

### 3.1 Basic results

To illustrate our analysis, we need the following three standard assumptions.

**Assumption 1.** (*Existence of  $f_{\rho}$* ) We assume  $f_{\rho} \in \mathcal{H}$ .

This is a standard assumption in learning theory and assumes that the target function  $f_{\rho}$  defined in Eq. (2.1) is indeed realizable, see also [RR19, RR17, CZ07, SS07].

**Assumption 2.** (*Noise condition [LR20, DW18]*) There exists  $\sigma$  such that  $\mathbb{E}[(f_{\rho}(\mathbf{x}) - y)^2 | \mathbf{x}] \leq \sigma^2$ , almost surely.

This is a broad model for the noise in the output  $y$ , containing uniformly bounded or sub-Gaussian noise; and is in fact weaker than the standard Bernstein condition, e.g., in [BK10].

**Assumption 3.** ( *$(8+m)$ -moments [LR20, LD20]*) Let  $\mathbf{x}_i = \Sigma_d^{1/2} \mathbf{t}_i$ , where  $\mathbf{t}_i \in \mathbb{R}^d$  has i.i.d. entries with zero mean, unit variance, and a finite  $(8+m)$ -moments, i.e., its entry  $\mathbf{t}_i(j)$ ,  $1 \leq j \leq d$ , satisfies  $\mathbb{E}[\mathbf{t}_i(j)] = 0$ ,  $\mathbb{V}[\mathbf{t}_i(j)] = 1$ , and  $\mathbb{E}[|\mathbf{t}_i(j)|^s] \leq C d^{\frac{s-2}{8+m}}$  such that  $\mathbb{E}[\mathbf{x}_i \mathbf{x}_i^{\top}] = \Sigma_d$  with a bounded spectral norm  $\|\Sigma_d\|_2$ , for some  $m > 0$ .

This is a standard setting in high-dimensional statistics and random matrix theory [EK10, DW18, LR20, HMRT19, EKZ<sup>+</sup>20] that assumes that the data are drawn from some not-too-heavy-tailed distribution, with possibly (involved) structure between the entries.

To aid our proof, we need some extra notations. In [EK10], it has been show that the kernel matrix  $\mathbf{K}$  in high dimension can be well approximated by  $\widetilde{\mathbf{K}}^{\text{lin}}$  in spectral norm, i.e.,  $\|\mathbf{K} - \widetilde{\mathbf{K}}^{\text{lin}}\|_2 \rightarrow 0$  as  $n, d \rightarrow \infty$

$$\widetilde{\mathbf{K}}^{\text{lin}} := \alpha \mathbf{1}\mathbf{1}^{\top} + \beta \frac{\mathbf{X}\mathbf{X}^{\top}}{d} + \gamma \mathbf{I} + \mathbf{T}, \quad (3.1)$$

**Table 2:** Parameters of the linearized kernel  $\widetilde{\mathbf{K}}^{\text{lin}}$  in [EK10].

parameters	inner-product kernels	radial kernels
$\alpha$	$h(0) + h''(0) \frac{\text{tr}(\boldsymbol{\Sigma}_d^2)}{2d^2}$	$h(2\tau) + 2h''(2\tau) \frac{\text{tr}(\boldsymbol{\Sigma}_d^2)}{d^2}$
$\beta$	$h'(0)$	$-2h'(2\tau)$
$\gamma$	$h(\tau) - h(0) - \tau h'(0)$	$h(0) + 2\tau h'(2\tau) - h(2\tau)$
$\mathbf{T}$	$\mathbf{0}_{n \times n}$	$h'(2\tau)\mathbf{A} + \frac{1}{2}h''(2\tau)\mathbf{A} \odot \mathbf{A}$ <sup>1</sup>

<sup>1</sup>  $\mathbf{A} := \mathbf{1}\boldsymbol{\psi}^\top + \boldsymbol{\psi}\mathbf{1}^\top$ , where  $\boldsymbol{\psi} \in \mathbb{R}^n$  with  $\psi_i := \|\mathbf{x}_i\|_2^2/d - \tau$  and  $\tau := \text{tr}(\boldsymbol{\Sigma}_d)/d$ .

with non-negative parameters  $\alpha, \beta, \gamma$ , and the additional matrix  $\mathbf{T}$  given in Table 2, see some typical examples in Appendix A. Here  $\gamma$  is the *implicit* regularization parameter in kernel estimator that depends on the nonlinear function  $h$  in the kernel  $k$  and the data structure  $\boldsymbol{\Sigma}_d$ . According to Eq. (3.1), denote the shortcut  $\widetilde{\mathbf{X}} := \beta\mathbf{X}\mathbf{X}^\top/d + \alpha\mathbf{1}\mathbf{1}^\top$ , we show in high dimension that,  $\mathbf{K}$  admits the same eigenvalue decay as  $\widetilde{\mathbf{X}}$  and  $\mathbf{X}\mathbf{X}^\top/d$  (see details in Appendix B). Subsequently, we introduce the following quantity function

$$\mathcal{N}_{\widetilde{\mathbf{X}}}^b := \text{tr} \left[ (\widetilde{\mathbf{X}} + b\mathbf{I}_n)^{-2} \widetilde{\mathbf{X}} \right] = \sum_{i=1}^n \frac{\lambda_i(\widetilde{\mathbf{X}})}{[b + \lambda_i(\widetilde{\mathbf{X}})]^2}, \quad (3.2)$$

which is associated with various quantity functions in [AKT19, DW18, LR20, JSS<sup>+</sup>20, NVKM20] and, as we shall see, plays an important role in determining the variance behavior. We will discuss at length  $\mathcal{N}_{\widetilde{\mathbf{X}}}^b$  based on different data eigenvalue decays in Section 4.

Formally, our main results of KRR in a high-dimensional regime are stated as follows.

**Theorem 1.** (*Basic result*) Under Assumptions 1-3, let  $0 < \delta < 1/2$ ,  $\theta = \frac{1}{2} - \frac{2}{8+m}$ ,  $d$  large enough, taking the regularization parameter  $\lambda := \bar{c}n^{-\vartheta}$  with  $0 \leq \vartheta \leq 1/2$ , for any given  $\varepsilon > 0$ , it holds with probability at least  $1 - 2\delta - d^{-2}$  with respect to the draw of  $\mathbf{X}$  that

$$\mathbb{E}_{y|\mathbf{x}} \|f_{z,\lambda} - f_\rho\|_{\mathcal{L}_{\rho_X}^2}^2 \lesssim n^{-\vartheta} \log^4\left(\frac{2}{\delta}\right) + \mathbf{V}_1 + \mathbf{V}_2, \quad (3.3)$$

with  $\mathbf{V}_1 := \frac{\sigma^2\beta}{d} \mathcal{N}_{\widetilde{\mathbf{X}}}^{n\lambda+\gamma}$  and the residual term  $\mathbf{V}_2$

$$\mathbf{V}_2 := \begin{cases} \frac{\sigma^2 \log^{2+4\varepsilon} d}{(n\lambda + \gamma)^2 d^{4\theta-1}}, & \text{for inner-product kernels} \\ \frac{\sigma^2}{(n\lambda + \gamma)^2} d^{-2\theta} \log^{1+\varepsilon} d, & \text{for radial kernels.} \end{cases}$$

**Remark:** The first term in Eq. (3.3) is the bound of the bias, which is independent of  $d$  and monotonically decreases with  $n$ . The sum  $\mathbf{V}_1 + \mathbf{V}_2$  is the bound of the variance that depends on both  $n$  and  $d$ . Note that  $\mathbf{V}_2$  monotonically decreases with  $n$ , and approaches to zero for a large  $n$ . Therefore, the error bound for  $\mathbf{V}_1 \asymp \frac{1}{d} \mathcal{N}_{\widetilde{\mathbf{X}}}^{n\lambda+\gamma}$  is the key part of estimates for the variance and will be discussed in Section 4, where  $n\lambda$  corresponds to the *explicit* regularization and  $\gamma$  the *implicit* regularization. We will demonstrate that  $\mathbf{V}_1$  can be monotonically decreasing or unimodal under different regularization schemes. Such monotonic bias and unimodal variance can lead to various behaviors of the excess risk, including monotonically decreasing, double descent, and bell-shaped risk curve, as illustrated in Figure 1 of introduction.

## 3.2 Refined result

Based on the basic result, if we consider two additional assumptions, i.e., extending Assumption 1 by considering the regularity of  $f_\rho$  and studying spectral decay of  $k$  via complexity of  $\mathcal{H}$ , we can obtain a refined result.

**Assumption 4.** (Source condition [CZ07])

$$f_\rho = L_K^r g_\rho, \quad \text{with some } 0 < r \leq 1 \text{ and } g_\rho \in \mathcal{L}_{\rho_X}^2 \text{ satisfying } \|g_\rho\|_{\mathcal{L}_{\rho_X}^2} \leq R .$$

It has been widely used in the literature of learning theory to assess the regularity of  $f_\rho$  [CZ07, ZDW13, RR17], which indicates  $f_\rho$  belongs to the range space of  $L_K^r$ . Assumption 1 is the worst case of Assumption 4 by choosing  $r = 1/2$  since  $\|f\|_{\mathcal{L}_{\rho_X}^2} = \|L_K^{1/2} f\|_{\mathcal{H}}, \forall f \in \mathcal{L}_{\rho_X}^2$ .

**Assumption 5.** (Capacity condition [CZ07]) For any  $\lambda > 0$ , there exist  $Q > 0$  and  $\eta \in [0, 1]$  such that

$$\mathcal{N}(\lambda) := \text{tr}((L_K + \lambda I)^{-1} L_K) \leq Q^2 \lambda^{-\eta} .$$

The notation  $\mathcal{N}(\lambda)$ , termed ‘‘effective dimension’’, is a quantity measuring the complexity of  $\mathcal{H}$  with respect to  $\rho_X$ , which can be regarded as a ‘‘measure of size’’ of the RKHS. This is a natural and widely used assumption in the literature [CZ07, ZDW13, RR17]. Assumption 5 always holds for  $\eta = 1$  and  $Q := \kappa$  where  $\kappa := \max\{1, \sup_{\mathbf{x} \in X} \sqrt{k(\mathbf{x}, \mathbf{x})}\}$  as  $L_K$  is a trace class operator. Its kernel matrix form is  $d_{\mathbf{K}}^\lambda := \text{tr}((\mathbf{K} + \lambda \mathbf{I}_n)^{-1} \mathbf{K}) = \sum_{i=1}^n \frac{\lambda_i(\mathbf{K})}{\lambda_i(\mathbf{K}) + \lambda}$  [AKM+17, LTOS19]. Since  $\frac{1}{n} \lambda_i(\mathbf{K})$  will converge to  $\mu_i$  in the limit as  $n \rightarrow \infty$  [STWCK02], we have  $\mathcal{N}(\lambda) \leq d_{\mathbf{K}}^\lambda$ . Further, according to the definition in Eq. (3.2), we can derive  $\mathcal{N}_{\mathbf{K}}^\lambda \leq d_{\mathbf{K}}^\lambda + \mathcal{O}(n/\lambda^2)$ . In fact, Assumption 5 can be substituted by investigating the eigenvalue decay of  $\mathbf{K}$ , see Section 4 for details. Based on the above discussion, we obtain a refined result of Theorem 1 as below.

**Theorem 2.** (Refined result) Under Assumptions 2-5, let  $0 < \delta < 1/2$ ,  $\theta = \frac{1}{2} - \frac{2}{8+m}$ , and  $d$  large enough, taking  $\lambda := \bar{c} n^{-\vartheta}$  with  $0 \leq \vartheta \leq \frac{1}{1+\eta}$ , then for any given  $\varepsilon > 0$ , it holds with probability at least  $1 - 2\delta - d^{-2}$

$$\mathbb{E}_{y|\mathbf{x}} \|f_{z,\lambda} - f_\rho\|_{\mathcal{L}_{\rho_X}^2}^2 \leq \widetilde{C}_1 n^{-2\vartheta r} \log^4\left(\frac{2}{\delta}\right) + \mathbf{V}_1 + \mathbf{V}_2, \quad (3.4)$$

where  $\mathbf{V}_1$  and  $\mathbf{V}_2$  are the same as in Theorem 1.

**Remark:** Compared to classical learning theory results [FS17] achieving  $\mathcal{O}(n^{-\frac{2r+1}{2r+1+\eta}})$  learning rates, the parameter  $\eta$  in our results only effects the selection range of  $\lambda$ , which is nearly independent of the learning rates to some extent. That means, the spectral decay of a kernel function  $k$  in high dimension is almost irrelevant to its kernel type. In fact, the eigenvalue decay of the kernel matrix in our model largely depends on the data, which is in essence different from classical learning theory results. Therefore, our result reflects a certain ‘‘universality’’ on the kernel function in high dimensional problems, which shows consistency to [EK10].

### 3.3 Compare to previous efforts

We provide non-asymptotic results that systematically analyze both implicit and explicit regularization schemes within a unified framework.

**Implicit regularization in kernel/linear interpolation:** Implicit regularization can be induced by minimum norm solutions in linear interpolation [DLM19, KLS20], or the curvature of the kernel function in kernel interpolation [LR20]. Compared to the risk curve of [LR20] converging to a non-zero constant, the risk curve in our results tends to zero when  $n \gg d$ . Therefore, in the double descent case, our result demonstrates that the minimum of the expected risk in the second descent is lower than the first descent; while the same claim cannot be obtained from [LR20]. Besides, our error bound for the bias achieves an optimal learning rate  $\mathcal{O}(\lambda)$  in a minimax case if we consider the basic  $f_\rho \in \mathcal{H}$  case, which can be faster than  $\mathcal{O}(n^{-1/2})$  in [PRDVR20].

**Explicit regularization in kernel/linear regression:** We provide non-asymptotic results that refine a series of asymptotic analyses, e.g., the Stieltjes transform approach in [HMRT19, EKZ+20, YYY+20] and the statistical mechanic approach in [CBP20]. In fact, by considering the limiting eigenvalue distribution of  $\mathbf{X}\mathbf{X}^\top/d$  via its Stieltjes transform  $\frac{1}{n} \mathcal{N}_{\mathbf{X}\mathbf{X}^\top/d}^b \approx m(-b) - bm'(-b)$ , for  $m(b)$  the solution to the popular Marčenko–Pastur equation [MP67], our error bound is able to recover [HMRT19, Theorem 5] with  $b := \lambda$  and isotropic features  $\boldsymbol{\Sigma}_d = \mathbf{I}_d$ . Finite sample analyses are often based on a finer control of the Stieltjes



transform [JSS<sup>+</sup>20] or the effective ranks as in [BLLT20, CL20]. However, when compared to them that consider Gaussian data [JSS<sup>+</sup>20, NVKM20], sub-Gaussian data [BLLT20, CL20, CC20], or Gaussian covariates [RMR20], the data distribution in our model is quite general. Besides, under some specific situations, the regularization parameter  $\lambda$  in linear regression can be negative [KLS20] or optimal tuned [NVKM20] so as to generalize well. Recent researches [GMMM19, LRZ19, BCP20] on kernel regression in  $n := \mathcal{O}(d^c)$  shows different trends.

### 3.4 Proof framework

The proof of our results is fairly technical and lengthy, and we briefly sketch some main ideas of Theorem 2 here. Note that, Theorem 1 is a special case of Theorem 2 by taking  $r = 1/2$  and  $\eta = 1$ . The modified error decomposition, the error bounds of variance for radial kernels, and estimates for bias are the main elements of novelty in the proof.

In order to estimate the error  $\mathbb{E}_{y|\mathbf{x}}\|f_{\mathbf{z},\lambda} - f_\rho\|$  in the  $\mathcal{L}_{\rho_X}^2$  space, we need the following intermediate functions. Define  $f_\lambda = (L_K + \lambda I)^{-1}L_K f_\rho$ , where  $I$  is the identity operator, then  $f_\lambda$  is actually the minimizer of the following problem  $f_\lambda = \operatorname{argmin}_{f \in \mathcal{H}} \left\{ \|f - f_\rho\|_{\mathcal{L}_{\rho_X}^2}^2 + \lambda \|f\|_{\mathcal{H}}^2 \right\}$ . Besides, by defining

$$f_{\mathbf{X},\lambda}(\mathbf{x}) = k(\mathbf{x}, \mathbf{X})^\top (\mathbf{K} + n\lambda \mathbf{I})^{-1} f_\rho(\mathbf{x}),$$

we have  $f_{\mathbf{X},\lambda} = (L_{K,\mathbf{X}} + \lambda I)^{-1}L_{K,\mathbf{X}} f_\rho$ . Accordingly, the variance-bias decomposition is stated in the following lemma, with proof deferred to Appendix C.

**Lemma 3.1.** *Let  $f_{\mathbf{z},\lambda}$  be the minimizer of problem (1.1),  $\mathbb{E}_{y|\mathbf{x}}\|f_{\mathbf{z},\lambda} - f_\rho\|_{\mathcal{L}_{\rho_X}^2}^2$  can be bounded by*

$$\begin{aligned} \mathbb{E}_{y|\mathbf{x}}\|f_{\mathbf{z},\lambda} - f_\rho\|_{\mathcal{L}_{\rho_X}^2}^2 &= \mathbf{B} + \mathbf{V} \\ &\leq 2 \left( \|f_{\mathbf{X},\lambda} - f_\lambda\|_{\mathcal{L}_{\rho_X}^2}^2 + \|f_\lambda - f_\rho\|_{\mathcal{L}_{\rho_X}^2}^2 \right) + \mathbf{V} \end{aligned}$$

where the bias  $\mathbf{B}$  is defined as

$$\mathbf{B} := \mathbb{E}_{\mathbf{x}}\|k(\mathbf{x}, \cdot)^\top (\mathbf{K} + n\lambda \mathbf{I})^{-1} f_\rho(\mathbf{X}) - f_\rho\|_{\mathcal{L}_{\rho_X}^2}^2, \quad (3.5)$$

where  $f_\rho(\mathbf{X}) = [f_\rho(\mathbf{x}_1), f_\rho(\mathbf{x}_1), \dots, f_\rho(\mathbf{x}_n)]^\top \in \mathbb{R}^n$  and the variance  $\mathbf{V}$  is defined as

$$\mathbf{V} := \mathbb{E}_{\mathbf{x},y}\|k(\mathbf{x}, \cdot)^\top (\mathbf{K} + n\lambda \mathbf{I})^{-1} \boldsymbol{\epsilon}\|_{\mathcal{L}_{\rho_X}^2}^2, \quad (3.6)$$

where  $\boldsymbol{\epsilon} := \mathbf{y} - f_\rho(\mathbf{X})$  satisfying  $\mathbb{E}_{y|\mathbf{x}}[\boldsymbol{\epsilon}] = 0$ .

It is clear that, the variance term does not depend on the target function  $f_\rho$ , and the bias is independent of the residual error  $\boldsymbol{\epsilon}$ . Proof for the bias  $\mathbf{B} \lesssim n^{-2\theta r} \log^4(\frac{2}{\delta})$  can be found in Appendix D. Proof for the variance  $\mathbf{V} \lesssim \mathbf{V}_1 + \mathbf{V}_2$  refers to Appendix E.

## 4 Discussion on Error Bounds

In this section, we discuss our Theorem 2 for different eigenvalue profiles of  $\widetilde{\mathbf{X}}$  in the two regimes of  $n < d$  and  $n > d$ . Since  $\mathbf{K}$  shares the same eigenvalue decay as  $\mathbf{X}\mathbf{X}^\top/d$  and  $\widetilde{\mathbf{X}}$  (see Proposition B.1 in Appendix B), we do not distinguish these two data matrices in eigenvalue decay in the subsequent description. We first focus on the variance  $\mathbf{V}$  that can be unimodal or monotonically decreasing with  $n$  under various regularization schemes. Subsequently, we investigate the total risk curve as the sum of bias and variance. Note that  $\widetilde{\mathbf{X}}$  has different numbers of non-zero eigenvalues under the two regimes, which plays a significant role in characterizing the different cases of our bounds. Here we denote  $r_* := \operatorname{rank}(\widetilde{\mathbf{X}}) \leq \min\{n, d\}$  which also includes the rank-deficient case.

**Table 3:** Three eigenvalue decays of  $\widetilde{\mathbf{X}}$ .

eigenvalue decay	$\lambda_i(\widetilde{\mathbf{X}})$	
	$i \leq r_*$	$i > r_*$
<i>harmonic decay</i>	$n/i$	0
<i>polynomial decay</i>	$ni^{-2a}$ with $a > 1/2$	
<i>exponential decay</i>	$ne^{-ai}$ with $a > 0$	

#### 4.1 Variance trend for $n < d$

We consider here three eigenvalue decays of  $\widetilde{\mathbf{X}}$  via the spectrum of  $\mathbf{K}$ : *harmonic*, *polynomial*, and *exponential decay* [Bac13, LTOS19].

**Proposition 4.1.** *Under the three eigenvalue decays in Table 3, denote  $r_* = \text{rank}(\widetilde{\mathbf{X}})$ , then the quantity function  $\mathcal{N}_{\widetilde{\mathbf{X}}}^b$  with  $b := n\lambda + \gamma$  can be bounded by*

- 1) *harmonic decay:*  $\mathcal{N}_{\widetilde{\mathbf{X}}}^b \leq \frac{n}{b^2} \ln \frac{n+(r_*+1)b}{n+b} = \mathcal{O}\left(\frac{n}{b^2}\right)$ .
- 2) *polynomial decay:*  $\mathcal{N}_{\widetilde{\mathbf{X}}}^b \leq \frac{\widetilde{C}}{2ab} \left(\frac{n}{b}\right)^{\frac{1}{2a}}$ , where  $\widetilde{C}$  is some constant.
- 3) *exponential decay:*  $\mathcal{N}_{\widetilde{\mathbf{X}}}^b \leq \frac{1}{a} \left( \frac{1}{b+ne^{-a(r_*+1)}} - \frac{1}{b+ne^{-a}} \right)$ .

**Proof** The proof can be found in Appendix F. □

According to Proposition 4.1, we summarize our results in Table 1 and discuss them as follows:

**Harmonic decay:**  $\mathbf{V}_1 \leq \mathcal{O}\left(\frac{n}{b^2d}\right)$ .

For  $\lambda = 0$ , i.e., the ridgeless case, we have  $b = \gamma = \mathcal{O}(1)$ , and  $\mathbf{V}_1 \leq \mathcal{O}\left(\frac{n}{d}\right)$ , which indicates  $\mathbf{V}_1$  increases with  $n$  in the  $n < d$  regime. For  $\lambda \neq 0$ , taking  $\lambda := \bar{c}n^{-\vartheta}$ , we have  $\mathbf{V}_1 \leq \mathcal{O}\left(\frac{n}{d(\bar{c}n^{1-\vartheta} + \gamma)^2}\right)$ . To investigate the monotonicity of  $g(n) := \frac{n}{d(\bar{c}n^{1-\vartheta} + \gamma)^2}$ , define

$$n_* := \left( \frac{\gamma}{2 - 2\vartheta - \bar{c}} \right)^{\frac{1}{1-\vartheta}},$$

we find that, a large  $\lambda$  leads to a small  $n_*$ . According to the relationship between  $r_*$ ,  $n_*$ , and  $d$ , we can conclude that (see Table 1 and the red curve in Figure 1(a)):

When  $\vartheta \geq \frac{1}{2(2-\bar{c})}$ ,  $\mathbf{V}_1$  will increase with  $n$  until  $n := r_*$  and then remain unchanged when  $r_* < n < d$ .

When  $\vartheta < \frac{1}{2(2-\bar{c})}$ , there are various trends as follows:

- 1) if  $d < n_*$ , this is the same as the  $\vartheta \geq \frac{1}{2(2-\bar{c})}$  case;
- 2) if  $r_* < n_* < d$ ,  $\mathbf{V}_1$  will increase with  $n$  until  $n := r_*$ , and then remain unchanged when  $r_* < n < d$ ;
- 3) if  $n_* < r_* < d$ ,  $\mathbf{V}_1$  will increase with  $n$  until  $n := n_*$  and then decrease with  $n$  until  $n := r_*$ , and stay unchanged on  $r_* < n < d$ ;
- 4) If  $n_* < c$  such that  $n > c$  always holds for some constant  $c$ , we have  $\mathbf{V}_1$  increases with  $n$  until  $n := r_*$ , and then stays unchanged on  $r_* < n < d$ . Remark that, for  $\gamma < 2 - 2\vartheta - \bar{c}$ , we have  $n_* < 1$  and thus  $n > n_*$ , so that  $\mathbf{V}_1$  always decreases with  $n$  until  $n := r_*$ .

**Polynomial decay:**  $\mathbf{V}_1 \leq \mathcal{O}\left(\frac{1}{bd} \left(\frac{n}{b}\right)^{\frac{1}{2a}}\right)$ .

Similar to the discussions above, by defining

$$n_* = \left( \frac{\gamma}{2a\bar{c}[1 - (1 + \frac{1}{2a})\vartheta]} \right)^{\frac{1}{1-\vartheta}},$$

we obtain results similar to the case of *harmonic decay* with different thresholds:  $\vartheta \geq (1 + \frac{1}{2a})^{-1}$  and  $\vartheta < (1 + \frac{1}{2a})^{-1}$ , see Table 1 for details.

**Exponential decay:**  $\mathbf{V}_1 \leq \frac{\widetilde{C}\beta}{ad} \left( \frac{1}{b+ne^{-a(r_*+1)}} - \frac{1}{b+ne^{-a}} \right)$ .

Here we consider the monotonicity of the function  $G(n) := \left( \frac{1}{b+ne^{-a(r_*+1)}} - \frac{1}{b+ne^{-a}} \right)$  with  $b := n\lambda + \gamma$  to study the trend of  $\mathbf{V}_1$  regarding to  $n$ . Let  $n_*$  be the solution of the equation  $G'(n) = 0$ , then we have the



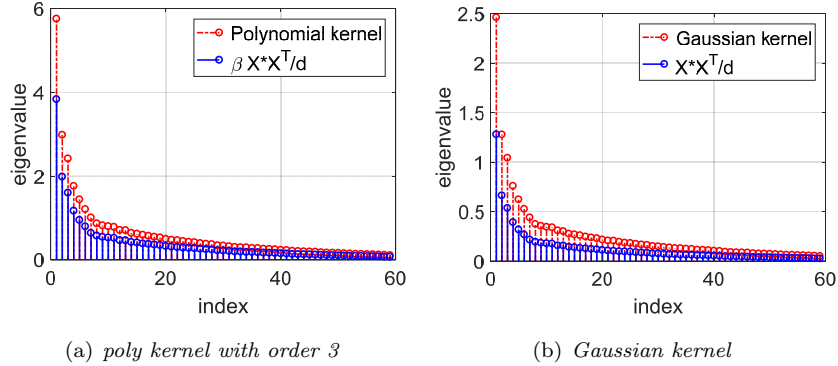


**Figure 2.** Top 60 eigenvalues of two kernel matrices and their linearizations on the subset of the *YearPredictionMSD* dataset. Note that the largest eigenvalue  $\lambda_1$  is not plotted for better display.

similar conclusion with that of *harmonic decay* and *polynomial decay* by the relationship between  $n_*$ ,  $r_*$ , and  $d$ , see Table 1 for details. More specifically, under some certain conditions,  $V_1$  is able to monotonically decrease with  $n$ , refer to Appendix F.1 for details.

## 4.2 Variance trends for $n > d$ and total risk

Different from the above  $n < d$  case, the current  $n > d$  regime admits that  $\widetilde{\mathbf{X}}$  has at most  $d$  non-zero eigenvalues. In this under-parameterized regime, we are particularly interested in the behavior as  $n \rightarrow \infty$ . In Appendix F.2, we prove that  $V_1$  approaches to zero as  $n \rightarrow \infty$  under the above three eigenvalue decays.

Based on the above discussions in the  $n > d$  and  $n < d$  regimes, we conclude that, the variance can be unimodal (small regularization) or decreasing (large regularization) as  $n$  grows, which, together with the fact that the bias is monotonically decreasing with  $n$ , leads to the following three configurations for the total risk: (i) if the bias dominates at small  $n$  and then decays fast (i.e., with a small regularization), we observe a double descent curve as in Figure 1(b); (ii) if the bias dominates but decays slowly (with a large regularization), the risk curve will be monotonic decreasing as in Figure 1(d); (iii) if the variance dominates, a bell-shaped risk curve as in Figure 1(c) will be observed.

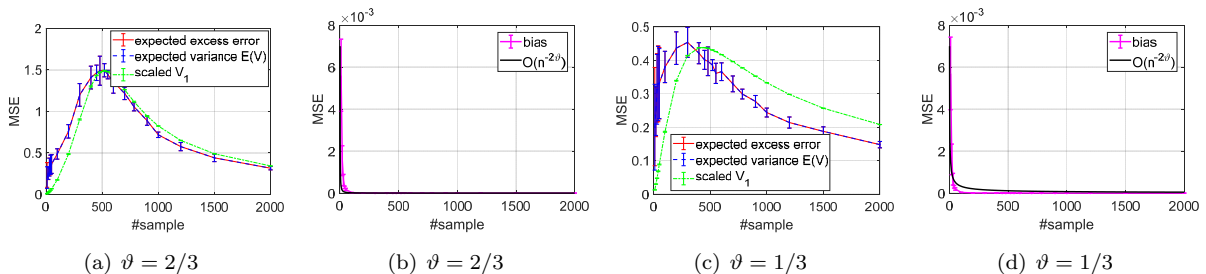


**Figure 3.** Harmonic decay of  $\widetilde{\mathbf{X}}$  with polynomial kernel: MSE of the expected excess risk, the variance in Eq. (3.6), our derived  $V_1$ , the bias in Eq. (3.5), and our derived convergence rate  $\mathcal{O}(n^{-2\vartheta r})$  with  $r = 1$  for different  $\vartheta$ .

## 5 Numerical Results

In this section, experiments are conducted to validate our theoretical results. Polynomial kernel of degree 3 and Gaussian kernel are evaluated on (i) a synthetic dataset that satisfies our technical assumptions and (ii) a subset of the *YearPredictionMSD* dataset [Cha08] with 1,000 data samples and  $d = 90$ , to study our derived error bounds for the bias and variance. More experimental results can be found in Appendix G.

**Eigenvalue decay equivalence:** Here we study the eigenvalue decay of the original polynomial/Gaussian kernel matrices and their linearization  $\mathbf{X}\mathbf{X}^T/d$  on the subset of *YearPredictionMSD* dataset. Note that,

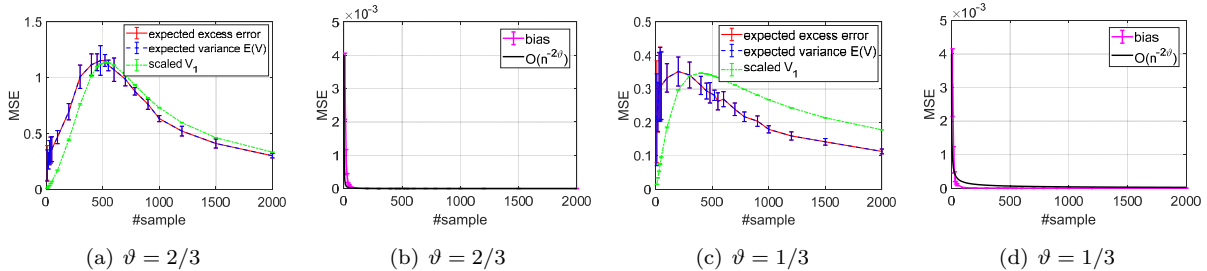


**Figure 4:** Harmonic decay of  $\widetilde{\mathbf{X}}$  in the Gaussian kernel case. The legend is the same as Figure 3.

polynomial kernels  $k(\mathbf{x}, \mathbf{x}') := (1 + \langle \mathbf{x}, \mathbf{x}' \rangle / d)^p$  admit  $\beta := p$  independent of  $\Sigma_d$  (see in Table 4), so we use the linearization  $\beta \mathbf{X} \mathbf{X}^\top / d$  for this kernel. Results in Figure 2 demonstrate that, the original nonlinear kernels admit the same eigenvalue decay as  $\mathbf{X} \mathbf{X}^\top / d$ . More experimental results on various dataset can be found in Appendix G.1.

**Risk curves on synthetic dataset:** To quantitatively assess our derived error bounds for the bias and variance, we generate a synthetic dataset under a known  $f_\rho$ , with *harmonic decay* for the data as an illustrating example. More experimental results on different eigenvalue decays refer to Appendix G.2. To be specific, we assume  $y_i = f_\rho(\mathbf{x}_i) + \varepsilon$  with target function  $f_\rho(\mathbf{x}) = \sin(\|\mathbf{x}\|_2^2)$  and Gaussian noise  $\varepsilon$  having zero-mean and unit-variance. The feature dimension  $d$  is set to 500. The samples are generated from  $\mathbf{x}_i = \Sigma_d^{1/2} \mathbf{t}_i$  (and thus  $\mathbf{X}^\top \mathbf{X} = \mathbf{T}^\top \Sigma_d \mathbf{T}$  with  $\mathbf{T} = [\mathbf{t}_1, \mathbf{t}_2, \dots, \mathbf{t}_n]^\top$ ) by the following steps:

- (i) take  $\Sigma_d$  as a diagonal matrix with its diagonal entries following with *harmonic decay*, i.e.,  $(\Sigma_d)_{ii} \propto n/i$ .
- (ii) take  $\mathbf{T}$  as a random orthogonal matrix<sup>1</sup> such that  $\mathbf{T}^\top \Sigma_d \mathbf{T}$  also has a harmonic eigendecay with  $\mathbf{T}$  having almost i.i.d entries.

Accordingly, the above generation process satisfies Assumption 3, and also  $\mathbf{X} \mathbf{X}^\top / d$  admits the same eigenvalue decay as  $\Sigma_d$ , which can be used to validate our discussion in Section 4. In this setting, the expected excess risk, the bias, and the variance can be directly (numerically) computed to validate our derived error bounds. The experimental results are validated across 10 trials. Specifically, to disentangle the *implicit regularization* effect of KRR on the final result, we apply the linearization of the polynomial/Gaussian kernel by setting  $\gamma = 0$  in Eq. (3.1). In this case, the explicit  $\lambda := \bar{c} n^{-\vartheta}$  is the only regularization in KRR. In our model,  $\bar{c}$  is empirically set to 0.01 to avoid a large  $\lambda$  when  $n$  is small.

Figures 3 and 4 show results under the *harmonic decay* setting for the linearization of the polynomial/Gaussian kernel, respectively. We observe that: 1) our error bound  $\mathbf{V}_1 \asymp \frac{1}{d} \mathcal{N}_{\widetilde{\mathbf{X}}}^{n, \lambda}$  exhibits the same trend as the true variance; 2) in this case, the variance dominates and we thus obtain a bell-shaped risk curve that first increases and then decreases; 3) as  $\vartheta$  decreases,  $\lambda$  increases and the peak point of the variance occurs at smaller and smaller  $n$ ; 4) the bias monotonically decreases with  $n$ , which corresponds to our error bound for the bias at a certain  $\mathcal{O}(n^{-2\vartheta r})$  rate in Theorem 2 by taking  $r = 1$  as the used  $f_\rho$  is smooth enough to achieve a good approximation error; 5) in our high-dimensional regimes, different kernels lead to the same convergence rates of the bias, which verifies our results but is different from those in classical learning theory.

**Risk curves on the real-world datasets:** Figure 5(a) shows the relative mean squared error (RMSE) of kernel ridgeless regression and its linearization in Eq. (3.1) on a subset (1,000 examples) of the *YearPredictionMSD* dataset averaged on 10 trials. Figure 5(b) shows the classification accuracy of such two methods on the *MNIST* dataset [LBBH98]. To evaluate the effectiveness of our error bounds, we plot the re-scaled  $\mathbf{V}_1 \asymp \frac{1}{d} \mathcal{N}_{\widetilde{\mathbf{X}}}^{n, \lambda}$  with  $\lambda = 0$ . It can be found that, kernel interpolation estimator generalizes well due to the *implicit regularization*, i.e.,  $\gamma \neq 0$ , which also exhibits a bell-shaped risk curve as our theoretical results suggest. However, in Figure 5(b), the risk curve monotonically decreases with  $n$  on the *MNIST* dataset [LBBH98], and at the same time kernel interpolation estimator and its linearization appear to generalize well. This observation may due to the *implicit regularization* parameter  $\gamma$  in Eq. (3.1) (of  $10^{-3}$  order on this dataset) that plays a fundamental role of “self-regularization”.

<sup>1</sup>We generate a random Gaussian matrix and use the QR decomposition to obtain the orthogonal matrix [YSC+16].

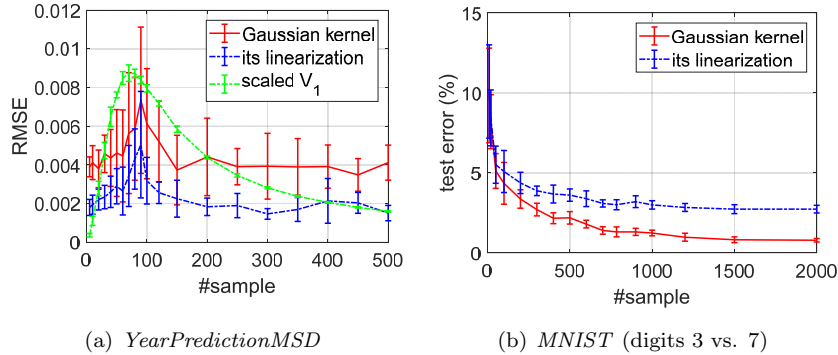


Figure 5: The test performance of the kernel interpolation estimator and its linearization one.

## 6 Conclusion

We derive non-asymptotic expressions for the expected excess risk of kernel ridge regression estimator in the under- and over-determined regime. The used linearization scheme of nonlinear smooth kernel allows us to discuss the *implicit* and *explicit* regularization on the risk curve. The provided refined analysis demonstrates that the monotonic bias and unimodal variance are able to exhibit various trends of risk curves. Since it is enough to require the kernel function differentiable in a neighborhood, our results can be further extended to the case of Laplace kernels [RZ19].

## Acknowledgement

This work was supported in part by the European Research Council under the European Union’s Horizon 2020 research and innovation program / ERC Advanced Grant E-DUALITY (787960). This paper reflects only the authors’ views and the Union is not liable for any use that may be made of the contained information; Research Council KUL C14/18/068; Flemish Government FWO project GOA4917N; Onderzoeksprogramma Artificiele Intelligentie (AI) Vlaanderen programme.

## References

- [AKM<sup>+</sup>17] Haim Avron, Michael Kapralov, Cameron Musco, Christopher Musco, Ameya Velingker, and Amir Zandieh, *Random Fourier features for kernel ridge regression: Approximation bounds and statistical guarantees*, Proceedings of the 34th International Conference on Machine Learning, 2017, pp. 253–262. 6
- [AKT19] Alnur Ali, J Zico Kolter, and Ryan J Tibshirani, *A continuous-time view of early stopping for least squares regression*, Proceedings of International Conference on Artificial Intelligence and Statistics, 2019, pp. 1370–1378. 1, 5
- [Bac13] Francis Bach, *Sharp analysis of low-rank kernel matrix approximations*, Proceedings of Conference on Learning Theory, 2013, pp. 185–209. 8
- [BCP20] Blake Bordelon, Abdulkadir Canatar, and Cengiz Pehlevan, *Spectrum dependent learning curves in kernel regression and wide neural networks*, Proceedings of International Conference on Machine Learning, 2020, pp. 1–11. 1, 7
- [BHMM19] Mikhail Belkin, Daniel Hsu, Siyuan Ma, and Soumik Mandal, *Reconciling modern machine-learning practice and the classical bias–variance trade-off*, Proceedings of the National Academy of Sciences **116** (2019), no. 32, 15849–15854. 1

- [BK10] Gilles Blanchard and Nicole Krämer, *Optimal learning rates for kernel conjugate gradient regression*, Proceedings of Advances in Neural Information Processing Systems, 2010, pp. 226–234. [4](#), [18](#)
- [BLLT20] Peter L. Bartlett, Philip M. Long, Gábor Lugosi, and Alexander Tsigler, *Benign overfitting in linear regression*, Proceedings of the National Academy of Sciences (2020). [1](#), [7](#)
- [BRT19] Mikhail Belkin, Alexander Rakhlin, and Alexandre B Tsybakov, *Does data interpolation contradict statistical optimality?*, Proceedings of International Conference on Artificial Intelligence and Statistics, 2019, pp. 1611–1619. [1](#)
- [CBP20] Abdulkadir Canatar, Blake Bordelon, and Cengiz Pehlevan, *Statistical mechanics of generalization in kernel regression*, arXiv preprint arXiv:2006.13198 (2020). [6](#)
- [CC20] Emmanuel Caron and Stephane Chretien, *A finite sample analysis of the double descent phenomenon for ridge function estimation*, arXiv preprint arXiv:2007.12882 (2020). [7](#)
- [Cha08] Chih-Chung Chang, *LibSVM data: Classification, regression, and multi-label*, <http://www.csie.ntu.edu.tw/~cjlin/libsvmtools/datasets/> (2008). [9](#)
- [CL20] Geoffrey Chinot and Matthieu Lerasle, *Benign overfitting in the large deviation regime*, arXiv preprint arXiv:2003.05838 (2020). [7](#)
- [CS02] Felipe Cucker and Steve Smale, *On the mathematical foundations of learning*, Bulletin of the American mathematical society **39** (2002), no. 1, 1–49. [1](#), [2](#)
- [CZ07] Felipe Cucker and Dingxuan Zhou, *Learning theory: an approximation theory viewpoint*, vol. 24, Cambridge University Press, 2007. [2](#), [3](#), [4](#), [6](#), [17](#)
- [DLM19] Michał Dereziński, Feynman Liang, and Michael W Mahoney, *Exact expressions for double descent and implicit regularization via surrogate random design*, arXiv preprint arXiv:1912.04533 (2019). [6](#)
- [DMDVR09] Christine De Mol, Ernesto De Vito, and Lorenzo Rosasco, *Elastic-net regularization in learning theory*, Journal of Complexity **25** (2009), no. 2, 201–230. [4](#)
- [DW18] Edgar Dobriban and Stefan Wager, *High-dimensional asymptotics of prediction: Ridge regression and classification*, Annals of Statistics **46** (2018), no. 1, 247–279. [4](#), [5](#)
- [EK10] Noureddine El Karoui, *The spectrum of kernel random matrices*, Annals of Statistics **38** (2010), no. 1, 1–50. [2](#), [4](#), [5](#), [6](#), [15](#), [16](#), [22](#), [23](#)
- [EKZ<sup>+</sup>20] Khalil Elkhailil, Abla Kammoun, Xiangliang Zhang, Mohamed-Slim Alouini, and Tareq Al-Naffouri, *Risk convergence of centered kernel ridge regression with large dimensional data*, IEEE Transactions on Signal Processing **68** (2020), 1574–1588. [2](#), [4](#), [6](#)
- [FS17] Simon Fischer and Ingo Steinwart, *Sobolev norm learning rates for regularized least-squares algorithm*, arXiv preprint arXiv:1702.07254 (2017). [6](#)
- [GMMM19] Behrooz Ghorbani, Song Mei, Theodor Misiakiewicz, and Andrea Montanari, *Linearized two-layers neural networks in high dimension*, arXiv preprint arXiv:1904.12191 (2019). [1](#), [7](#)
- [GSW17] Zheng-Chu Guo, Lei Shi, and Qiang Wu, *Learning theory of distributed regression with bias corrected regularization kernel network*, Journal of Machine Learning Research **18** (2017), no. 1, 4237–4261. [18](#)
- [HMRT19] Trevor Hastie, Andrea Montanari, Saharon Rosset, and Ryan J. Tibshirani, *Surprises in high-dimensional ridgeless least squares interpolation*, arXiv preprint arXiv:1903.08560 (2019). [1](#), [3](#), [4](#), [6](#), [29](#)

- [HRS16] Moritz Hardt, Ben Recht, and Yoram Singer, *Train faster, generalize better: Stability of stochastic gradient descent*, Proceedings of International Conference on Machine Learning, 2016, pp. 1225–1234. [1](#)
- [JSS<sup>+</sup>20] Arthur Jacot, Berfin Şimşek, Francesco Spadaro, Clément Hongler, and Franck Gabriel, *Kernel alignment risk estimator: Risk prediction from training data*, Proceedings of Advances in Neural Information Processing Systems, 2020, pp. 1–9. [5](#), [7](#)
- [KLS20] Dmitry Kobak, Jonathan Lomond, and Benoit Sanchez, *The optimal ridge penalty for real-world high-dimensional data can be zero or negative due to the implicit ridge regularization*, Journal of Machine Learning Research **21** (2020), no. 169, 1–16. [6](#), [7](#)
- [LBBH98] Yann Lecun, Leon Bottou, Yoshua Bengio, and Patrick Haffner, *Gradient-based learning applied to document recognition*, Proceedings of the IEEE **86** (1998), no. 11, 2278–2324. [10](#), [27](#)
- [LD20] Sifan Liu and Edgar Dobriban, *Ridge regression: Structure, cross-validation, and sketching*, Proceedings of International Conference on Learning Representations, 2020. [4](#)
- [LGZ17] Shao-Bo Lin, Xin Guo, and Ding-Xuan Zhou, *Distributed learning with regularized least squares*, Journal of Machine Learning Research **18** (2017), no. 1, 3202–3232. [17](#), [18](#)
- [Li20] Weilin Li, *Generalization error of minimum weighted norm and kernel interpolation*, arXiv preprint arXiv:2008.03365 (2020). [1](#)
- [LJB20] Daniel LeJeune, Hamid Javadi, and Richard Baraniuk, *The implicit regularization of ordinary least squares ensembles*, Proceedings of International Conference on Artificial Intelligence and Statistics, 2020, pp. 3525–3535. [1](#)
- [LR20] Tengyuan Liang and Alexander Rakhlin, *Just interpolate: Kernel “ridgeless” regression can generalize*, Annals of Statistics **48** (2020), no. 3, 1329–1347. [1](#), [2](#), [3](#), [4](#), [5](#), [6](#), [20](#), [23](#)
- [LRZ19] Tengyuan Liang, Alexander Rakhlin, and Xiyu Zhai, *On the multiple descent of minimum-norm interpolants and restricted lower isometry of kernels*, Proceedings of Annual Conference on Learning Theory, 2019, pp. 1–32. [7](#)
- [LTOS19] Zhu Li, Jean-Francois Ton, Dino Ogljic, and Dino Sejdinovic, *Towards a unified analysis of random Fourier features*, Proceedings of the 36th International Conference on Machine Learning, 2019, pp. 3905–3914. [6](#), [8](#)
- [MM19] Song Mei and Andrea Montanari, *The generalization error of random features regression: Precise asymptotics and double descent curve*, arXiv preprint arXiv:1908.05355 (2019). [1](#)
- [MP67] Vladimir A Marčenko and Leonid Andreevich Pastur, *Distribution of eigenvalues for some sets of random matrices*, Mathematics of the USSR-Sbornik **1** (1967), no. 4, 457. [6](#)
- [NVKM20] Preetum Nakkiran, Prayaag Venkat, Sham Kakade, and Tengyu Ma, *Optimal regularization can mitigate double descent*, arXiv preprint arXiv:2003.01897 (2020). [5](#), [7](#)
- [PRDVR20] Nicolò Pagliana, Alessandro Rudi, Ernesto De Vito, and Lorenzo Rosasco, *Interpolation and learning with scale dependent kernels*, arXiv preprint arXiv:2006.09984 (2020). [6](#)
- [RCR13] Alessandro Rudi, Guillermo D Canas, and Lorenzo Rosasco, *On the sample complexity of subspace learning*, Proceedings of Advances in Neural Information Processing Systems, 2013, pp. 2067–2075. [18](#)
- [RMR20] Dominic Richards, Jaouad Mourtada, and Lorenzo Rosasco, *Asymptotics of ridge (less) regression under general source condition*, arXiv preprint arXiv:2006.06386 (2020). [7](#)

- [RR17] Alessandro Rudi and Lorenzo Rosasco, *Generalization properties of learning with random features*, Proceedings of Advances in Neural Information Processing Systems, 2017, pp. 3215–3225. [4](#), [6](#), [18](#)
- [RR19] Dominic Richards and Patrick Rebeschini, *Optimal statistical rates for decentralised non-parametric regression with linear speed-up*, Advances in Neural Information Processing Systems, 2019, pp. 1216–1227. [4](#)
- [RZ19] Alexander Rakhlin and Xiyu Zhai, *Consistency of interpolation with laplace kernels is a high-dimensional phenomenon*, Proceedings of Conference on Learning Theory, 2019, pp. 2595–2623. [11](#)
- [SA08] Ingo Steinwart and Christmann Andreas, *Support vector machines*, Springer Science and Business Media, 2008. [4](#)
- [SHK<sup>+</sup>14] Nitish Srivastava, Geoffrey Hinton, Alex Krizhevsky, Ilya Sutskever, and Ruslan Salakhutdinov, *Dropout: a simple way to prevent neural networks from overfitting*, Journal of Machine Learning Research **15** (2014), no. 1, 1929–1958. [1](#)
- [SS07] Ingo Steinwart and Clint Scovel, *Fast rates for support vector machines using Gaussian kernels*, Annals of Statistics **35** (2007), no. 2, 575–607. [3](#), [4](#)
- [SSM97] Bernhard Schölkopf, Alexander J. Smola, and Klaus-Robert Müller, *Kernel principal component analysis*, Proceedings of International Conference on Artificial Neural Networks, 1997, pp. 583–588. [2](#)
- [STWCK02] John Shawe-Taylor, Chris Williams, Nello Cristianini, and Jaz Kandola, *On the eigenspectrum of the gram matrix and its relationship to the operator eigenspectrum*, Proceedings of International Conference on Algorithmic Learning Theory, Springer, 2002, pp. 23–40. [6](#)
- [SVGDB<sup>+</sup>02] Johan A.K. Suykens, Tony Van Gestel, Jos De Brabanter, Bart De Moor, and Joos Vandewalle, *Least squares support vector machines*, World Scientific, 2002. [2](#)
- [SZ07] Steve Smale and Ding-Xuan Zhou, *Learning theory estimates via integral operators and their approximations*, Constructive approximation **26** (2007), no. 2, 153–172. [17](#)
- [Wen04] Holger Wendland, *Scattered data approximation*, vol. 17, Cambridge university press, 2004. [1](#)
- [WZ11] Cheng Wang and Ding-Xuan Zhou, *Optimal learning rates for least squares regularized regression with unbounded sampling*, Journal of Complexity **27** (2011), no. 1, 55–67. [3](#)
- [YSC<sup>+</sup>16] Felix Xinnan Yu, Ananda Theertha Suresh, Krzysztof Choromanski, Daniel Holtmannrice, and Sanjiv Kumar, *Orthogonal random features*, Proceedings of Advances in Neural Information Processing Systems, 2016, pp. 1975–1983. [10](#)
- [YYY<sup>+</sup>20] Zitong Yang, Yaodong Yu, Chong You, Jacob Steinhardt, and Yi Ma, *Rethinking bias-variance trade-off for generalization of neural networks*, Proceedings of the International Conference on Machine Learning, 2020. [3](#), [6](#)
- [ZBH<sup>+</sup>16] Chiyuan Zhang, Samy Bengio, Moritz Hardt, Benjamin Recht, and Oriol Vinyals, *Understanding deep learning requires rethinking generalization*, arXiv preprint arXiv:1611.03530 (2016). [1](#)
- [ZDW13] Yuchen Zhang, John Duchi, and Martin Wainwright, *Divide and conquer kernel ridge regression*, Proceedings of Conference on Learning Theory, 2013, pp. 592–617. [6](#)



In this paper, Appendix is organized as follows.

- Section A provides high dimensional linearizations of some typical smooth kernels as concrete examples of Table 2.
- In Section B, we demonstrate that, a kernel matrix in high dimension admits the same eigenvalue decay as  $\widetilde{\mathbf{X}}$  and  $\mathbf{X}\mathbf{X}^\top/d$ .
- Our proof framework includes the error decomposition in Section C, the error bound for the bias in Section D and for the variance in Section E, respectively.
- Section F discusses the quantity function  $\mathcal{N}_{\widetilde{\mathbf{X}}}^{n\lambda+\gamma}$  based on three eigenvalue decays: *harmonic decay*, *polynomial decay*, and *exponential decay* in the  $n < d$  and  $n > d$  regimes.
- Some additional experiments are presented in Section G to further validate our theoretical results.

## A Examples of kernels and their linearizations

In this section, we present linearization of some typical kernels by Eq. (3.1). Here we assume that  $\alpha, \beta, \gamma \geq 0$  to ensure the positive definiteness of the approximated kernel matrix  $\widetilde{\mathbf{K}}^{\text{lin}}$ . Table 4 reports the results of three inner-product kernels including polynomial kernel, linear kernel, exponential kernel; as well as a radial kernel: the common-used Gaussian kernel. We can find that  $\alpha, \gamma \geq 0$ . Specifically,  $\beta > 0$  avoids a trivial solution.

**Table 4:** Linearizations of typical kernels in high dimension.

kernel	formulation	$\alpha$	$\beta$	$\gamma$
polynomial kernels	$k(\mathbf{x}, \mathbf{x}') := (1 + \frac{1}{d} \langle \mathbf{x}, \mathbf{x}' \rangle)^p$	$1 + p(p-1) \frac{\text{tr}(\boldsymbol{\Sigma}_d^2)}{2d^2}$	$p$	$(1 + \tau)^p - 1 - p\tau$
linear kernel	$k(\mathbf{x}, \mathbf{x}') = \frac{1}{d} \langle \mathbf{x}, \mathbf{x}' \rangle$	0	1	0
exponential kernel	$k(\mathbf{x}, \mathbf{x}') = \exp(\frac{2}{d} \langle \mathbf{x}, \mathbf{x}' \rangle)$	$1 + 2 \frac{\text{tr}(\boldsymbol{\Sigma}_d^2)}{d^2}$	2	$\exp(2\tau) - 1 - 2\tau$
Gaussian kernel	$k(\mathbf{x}, \mathbf{x}') = \exp(-\frac{1}{d} \ \mathbf{x} - \mathbf{x}'\ _2^2)$	$\exp(-2\tau) \left[ 1 + 2 \frac{\text{tr}(\boldsymbol{\Sigma}_d^2)}{d^2} \right]$	$2 \exp(-2\tau)$	$1 - 2\tau \exp(-2\tau) - \exp(-2\tau)$

## B Eigenvalue decay equivalence

In this section, we demonstrate that, in high dimension, a kernel matrix induced by inner-product kernels or radial kernels admits the same eigenvalue decay as  $\widetilde{\mathbf{X}} = \beta \mathbf{X}\mathbf{X}^\top/d + \alpha \mathbf{1}\mathbf{1}^\top$  and  $\mathbf{X}\mathbf{X}^\top/d$ .

For notational simplicity, denote the inner-product kernel matrix  $\mathbf{K}_{\text{inner}}$  and its linearization  $\widetilde{\mathbf{K}}_{\text{inner}}^{\text{lin}}$ ; the radial kernel matrix  $\mathbf{K}_{\text{radial}}$  and its linearization  $\widetilde{\mathbf{K}}_{\text{radial}}^{\text{lin}}$ .

**Proposition B.1.** *The inner-product kernel matrix  $\mathbf{K}_{\text{inner}}$  admits the same eigenvalue decay as  $\widetilde{\mathbf{X}}$  and  $\mathbf{X}\mathbf{X}^\top/d$ .*

**Proof** According to Theorem 2.1 in [EK10], the inner-product kernel matrix  $\mathbf{K}_{\text{inner}}$  can be well approximated by  $\widetilde{\mathbf{K}}_{\text{inner}}^{\text{lin}}$  with

$$\widetilde{\mathbf{K}}_{\text{inner}}^{\text{lin}} := \beta \frac{\mathbf{X}\mathbf{X}^\top}{d} + \gamma \mathbf{I} + \alpha \mathbf{1}\mathbf{1}^\top,$$

in a spectral norm sense, where  $\alpha, \beta, \gamma$  are given in Table 2. As a result, with high probability, the inner-product kernel matrix  $\mathbf{K}_{\text{inner}}$  and its linearization  $\widetilde{\mathbf{K}}_{\text{inner}}^{\text{lin}}$  has the same eigenvalue. That means,  $\mathbf{K}_{\text{inner}}$  admits the same eigenvalue decay as  $\widetilde{\mathbf{X}} := \beta \mathbf{X}\mathbf{X}^\top/d + \alpha \mathbf{1}\mathbf{1}^\top$  via a constant shift  $\gamma$ .



Next, we shall demonstrate that  $\mathbf{K}_{\text{inner}}$  admits the same eigenvalue decay as  $\mathbf{X}\mathbf{X}^\top/d$ . Since  $\mathbf{1}\mathbf{1}^\top$  is a rank-one matrix with  $\lambda_1(\mathbf{1}\mathbf{1}^\top) = n$ , with Weyl's inequality and  $\lambda_n \leq \lambda_{n-1} \leq \dots \leq \lambda_1$ , we have

$$\beta\lambda_1\left(\frac{\mathbf{X}\mathbf{X}^\top}{d}\right) + \gamma \leq \lambda_1(\widetilde{\mathbf{K}}_{\text{inner}}^{\text{lin}}) \leq \beta\lambda_1\left(\frac{\mathbf{X}\mathbf{X}^\top}{d}\right) + \gamma + \alpha n,$$

and

$$\beta\lambda_i\left(\frac{\mathbf{X}\mathbf{X}^\top}{d}\right) + \gamma \leq \lambda_i(\widetilde{\mathbf{K}}_{\text{inner}}^{\text{lin}}) \leq \beta\lambda_{i-1}\left(\frac{\mathbf{X}\mathbf{X}^\top}{d}\right) + \gamma, \quad i = 2, 3, \dots, n,$$

so that the eigenvalue of  $\widetilde{\mathbf{K}}_{\text{inner}}^{\text{lin}}$  interlaced with those of  $\beta\mathbf{X}\mathbf{X}^\top/d + \gamma\mathbf{I}$ . We can thus conclude that the eigenvalue decay of  $\widetilde{\mathbf{K}}_{\text{inner}}^{\text{lin}}$  is the same as that of  $\mathbf{X}\mathbf{X}^\top/d$  with a constant shift and scaling, which do not effect the trend of eigenvalue decay. Accordingly, the inner-product-type kernel matrix  $\mathbf{K}_{\text{inner}}$  and its linearization  $\widetilde{\mathbf{K}}_{\text{inner}}^{\text{lin}}, \widetilde{\mathbf{X}}$  admit the same eigenvalue decay as  $\mathbf{X}\mathbf{X}^\top/d$ , which concludes the proof.  $\square$

Proposition B.1 also provides a justification to study the eigenvalue decay of a radial kernel matrix. According to Theorem 2.2 in [EK10], the radial kernel matrix  $\mathbf{K}_{\text{radial}}$  can be well approximated by  $\widetilde{\mathbf{K}}_{\text{radial}}^{\text{lin}}$  with

$$\widetilde{\mathbf{K}}_{\text{radial}}^{\text{lin}} := \beta\frac{\mathbf{X}\mathbf{X}^\top}{d} + \gamma\mathbf{I} + \alpha\mathbf{1}\mathbf{1}^\top + h'(2\tau)\mathbf{A} + \frac{1}{2}h''(2\tau)\mathbf{A} \odot \mathbf{A},$$

in a spectral norm sense, where  $\alpha, \beta, \gamma$  are given in Table 2. Recall  $\mathbf{A} := \mathbf{1}\boldsymbol{\psi}^\top + \boldsymbol{\psi}\mathbf{1}^\top$ , where  $\boldsymbol{\psi} \in \mathbb{R}^n$  with  $\psi_i := \|\mathbf{x}_i\|_2^2/d - \tau$ , we find that  $\mathbf{A}$  is a rank 2 matrix with its eigenvalues  $\lambda(\mathbf{A}) = \mathbf{1}^\top\boldsymbol{\psi} \pm \sqrt{n}\|\boldsymbol{\psi}\|_2$ , and thus we have  $\text{rank}(\mathbf{A} \odot \mathbf{A}) = 3$ .<sup>2</sup> Hence, by virtue of Proposition B.1, apart from the top 5 eigenvalues of the radial kernel matrix  $\mathbf{K}_{\text{radial}}$ , its remaining eigenvalues follow with

$$\beta\lambda_i\left(\frac{\mathbf{X}\mathbf{X}^\top}{d}\right) + \gamma \leq \lambda_i(\widetilde{\mathbf{K}}_{\text{radial}}^{\text{lin}}) \leq \beta\lambda_{i-1}\left(\frac{\mathbf{X}\mathbf{X}^\top}{d}\right) + \gamma, \quad i = 6, 7, \dots, n.$$

Accordingly,  $\mathbf{K}_{\text{radial}}$  admits the same eigenvalue decay as  $\mathbf{X}\mathbf{X}^\top/d$ .

## C Proof of Lemma 3.1

**Proof** By virtue of the closed form of the KRR estimator in Eq. (2.2) and  $\boldsymbol{\epsilon} := \mathbf{y} - f_\rho(\mathbf{X})$ , we have

$$f_{\mathbf{z},\lambda}(\mathbf{x}) - f_\rho(\mathbf{x}) = k(\mathbf{x}, \mathbf{X})^\top (\mathbf{K} + n\lambda\mathbf{I})^{-1} \boldsymbol{\epsilon} + k(\mathbf{x}, \mathbf{X})^\top (\mathbf{K} + n\lambda\mathbf{I})^{-1} f_\rho(\mathbf{X}) - f_\rho(\mathbf{x}),$$

where  $f_\rho(\mathbf{X}) = [f_\rho(\mathbf{x}_1), f_\rho(\mathbf{x}_1), \dots, f_\rho(\mathbf{x}_n)]^\top \in \mathbb{R}^n$ . According to  $\mathbb{E}_{y|\mathbf{x}}[\boldsymbol{\epsilon}] = 0$ , we then have

$$\mathbb{E}_{y|\mathbf{x}} \|f_{\mathbf{z},\lambda} - f_\rho\|_{\mathcal{L}_{\rho_X}^2}^2 = \mathbb{E}_{\mathbf{x}} \|k(\mathbf{x}, \cdot)^\top (\mathbf{K} + n\lambda\mathbf{I})^{-1} f_\rho(\mathbf{X}) - f_\rho\|_{\mathcal{L}_{\rho_X}^2}^2 + \mathbb{E}_{y,\mathbf{x}} \|k(\mathbf{x}, \cdot)^\top (\mathbf{K} + n\lambda\mathbf{I})^{-1} \boldsymbol{\epsilon}\|_{\mathcal{L}_{\rho_X}^2}^2.$$

Based on the definition of  $\mathbf{B}$ , we decompose  $\mathbf{B}$  as

$$\begin{aligned} \mathbf{B} &:= \mathbb{E}_{\mathbf{x}} \|k(\mathbf{x}, \cdot)^\top (\mathbf{K} + n\lambda\mathbf{I})^{-1} f_\rho(\mathbf{X}) - f_\rho\|_{\mathcal{L}_{\rho_X}^2}^2 = \|f_{\mathbf{X},\lambda} - f_\rho\|_{\mathcal{L}_{\rho_X}^2}^2 \\ &\leq 2\|f_{\mathbf{X},\lambda} - f_\lambda\|_{\mathcal{L}_{\rho_X}^2}^2 + 2\|f_\lambda - f_\rho\|_{\mathcal{L}_{\rho_X}^2}^2, \end{aligned}$$

which concludes our proof.  $\square$

<sup>2</sup>This can be proved using rank-one decomposition of  $\mathbf{A}$ .

## D Proof for the bias

The error bound for the bias is given by the following theorem.

**Theorem 3.** (*Bias*) Under Assumption 4 (source condition with  $0 < r \leq 1$ ), Assumption 5 (capacity condition with  $0 \leq \eta \leq 1$ ), let  $0 < \delta < 1/2$ , taking the regularization parameter  $\lambda := \bar{c}n^{-\vartheta}$  with  $0 \leq \vartheta \leq \frac{1}{1+\eta}$ , there holds with probability at least  $1 - 2\delta$ , we have

$$\mathbb{B} \leq 2 \left( \|f_{\mathbf{X},\lambda} - f_\lambda\|_{\mathcal{L}_{\rho_{\mathbf{X}}}^2}^2 + \|f_\lambda - f_\rho\|_{\mathcal{L}_{\rho_{\mathbf{X}}}^2}^2 \right) \lesssim n^{-2\vartheta r} \log^4 \left( \frac{2}{\delta} \right).$$

In our error decomposition,  $\|f_\lambda - f_\rho\|_{\mathcal{L}_{\rho_{\mathbf{X}}}^2}^2$  is independent of data  $\mathbf{X}$  that corresponds to the approximation error in learning theory [CZ07]; while the first term  $\|f_{\mathbf{X},\lambda} - f_\lambda\|_{\mathcal{L}_{\rho_{\mathbf{X}}}^2}^2$  depends on  $\mathbf{X}$ , termed as bias-sample error. To prove Theorem 3, we need to bound the approximation error and the bias-sample error as follows.

### D.1 Bound approximation error

In learning theory, the approximation error  $\|f_\lambda - f_\rho\|_{\mathcal{L}_{\rho_{\mathbf{X}}}^2}$  can be estimated by the source condition in Assumption 4.

**Lemma D.1.** (*Lemma 3 in [SZ07]*) Under the source condition in Assumption 4 with  $0 < r \leq 1$ , the approximation error can be given by

$$\|f_\lambda - f_\rho\|_{\mathcal{L}_{\rho_{\mathbf{X}}}^2} = \|(L_K + \lambda I)^{-1} L_K f_\rho - f_\rho\|_{\mathcal{L}_{\rho_{\mathbf{X}}}^2} \leq \lambda^r \|L_K^{-r} f_\rho\|_{\mathcal{L}_{\rho_{\mathbf{X}}}^2} \leq R\lambda^r.$$

### D.2 Bound bias-sample error

To bound the bias-sample error  $\|f_{\mathbf{X},\lambda} - f_\lambda\|_{\mathcal{L}_{\rho_{\mathbf{X}}}^2}$ , we need the following lemma.

**Lemma D.2.** (*Lemma 17 in [LGZ17]*) For any  $0 < \delta < 1$ , it holds with probability at least  $1 - \delta$  that

$$\|(L_K + \lambda I)^{-1/2} (L_K - L_{K,\mathbf{X}})\| \leq \frac{2\kappa}{\sqrt{n}} \left\{ \frac{\kappa}{\sqrt{n\lambda}} + \sqrt{\mathcal{N}(\lambda)} \right\} \log \left( \frac{2}{\delta} \right),$$

where  $\kappa := \max\{1, \sup_{\mathbf{x} \in X} \sqrt{k(\mathbf{x}, \mathbf{x})}\}$ .

Then the bias-sample error can be decomposed into several parts.

**Lemma D.3.** Under Assumption 4, we have

$$\begin{aligned} \|f_{\mathbf{X},\lambda} - f_\lambda\| &\leq R\lambda^{1/2} \|(L_{K,\mathbf{X}} + \lambda I)^{-1/2} (L_K + \lambda I)^{1/2}\| \|(L_K + \lambda I)^{-1/2} (L_K - L_{K,\mathbf{X}})\|^r \\ &\quad \|(L_K + \lambda I)^{-1/2} (L_K - L_{K,\mathbf{X}}) (L_K + \lambda I)^{-1}\|^{1-r}. \end{aligned}$$

**Proof** [Proof of Lemma D.3] According to the definition of  $f_{\mathbf{X},\lambda}$  and  $f_\lambda$ , we have

$$f_{\mathbf{X},\lambda} - f_\lambda = (L_{K,\mathbf{X}} + \lambda I)^{-1} L_{K,\mathbf{X}} f_\rho - (L_K + \lambda I)^{-1} L_K f_\rho.$$

Due to  $(A + \lambda I)^{-1} A = I - \lambda(A + \lambda I)^{-1}$  for any bounded positive operator  $A$ , we have

$$(L_K + \lambda I)^{-1} L_K f_\rho - (L_{K,\mathbf{X}} + \lambda I)^{-1} L_{K,\mathbf{X}} f_\rho = \lambda \left[ (L_{K,\mathbf{X}} + \lambda I)^{-1} - (L_K + \lambda I)^{-1} \right] f_\rho.$$

Further, by virtue of the first order decomposition of operator difference:  $A^{-1} - B^{-1} = A^{-1}(B - A)B^{-1}$  for any invertible bounded operator and using the source condition in Assumption 4, the above equation can be further expressed as

$$\begin{aligned} (L_K + \lambda I)^{-1} L_K f_\rho - (L_{K,\mathbf{X}} + \lambda I)^{-1} L_{K,\mathbf{X}} f_\rho &= \lambda (L_{K,\mathbf{X}} + \lambda I)^{-1} (L_K - L_{K,\mathbf{X}}) (L_K + \lambda I)^{-1} L_K^r g_\rho \\ &= \lambda^{1/2} \left( \lambda^{1/2} (L_{K,\mathbf{X}} + \lambda I)^{-1/2} \right) \left( (L_{K,\mathbf{X}} + \lambda I)^{-1/2} (L_K + \lambda I)^{1/2} \right) \\ &\quad \left( (L_K + \lambda I)^{-1/2} (L_K - L_{K,\mathbf{X}}) (L_K + \lambda I)^{-(1-r)} \right) \left( (L_K + \lambda I)^{-r} L_K^r \right) g_\rho. \end{aligned}$$

Besides, using  $\|AB^t\| \leq \|A\|^{1-t}\|AB\|^t$  with  $t \in [0, 1]$  for any bounded linear operator  $A$  and positive semi-definite operator  $B$  in Proposition 9 in [RR17], we have

$$\begin{aligned} \|(L_K + \lambda I)^{-1/2}(L_K - L_{K,\mathbf{X}})(L_K + \lambda I)^{-(1-r)}\| &\leq \|(L_K + \lambda I)^{-1/2}(L_K - L_{K,\mathbf{X}})\|^r \\ &\quad \|(L_K + \lambda I)^{-1/2}(L_K - L_{K,\mathbf{X}})(L_K + \lambda I)^{-1}\|^{1-r}, \end{aligned}$$

where we choose  $A := (L_K + \lambda I)^{-1/2}(L_K - L_{K,\mathbf{X}})$ ,  $B := (L_K + \lambda I)^{-1}$ , and  $t := 1 - r \in [0, 1]$ . Accordingly, we can conclude our proof due to  $\|(L_{K,\mathbf{X}} + \lambda I)^{-1/2}\| \leq 1/\sqrt{\lambda}$  and  $\|(L_K + \lambda I)^{-r}L_{K,\mathbf{X}}^r\| \leq 1$ .  $\square$

**Remark:** The proof framework of Lemma D.3 is similar to Lemma 4 in [RR17] but we consider a more general case  $0 < r \leq 1$  than  $1/2 \leq r \leq 1$  in [RR17]. Although  $0 < r < 1/2$  appears to be unattainable as claimed in [RR17], we follow with [LGZ17, GSW17] on a quite general case with  $r > 0$ .

To prove Theorem 3, we also need the following two lemmas.

**Lemma D.4.** (Proposition 6 in [RR17]) Let  $\delta \in (0, 1/2]$ , it holds with probability at least  $1 - 2\delta$  that

$$\begin{aligned} &\|(L_K + \lambda I)^{-1/2}(L_K - L_{K,\mathbf{X}})(L_K + \lambda I)^{-1}\| \\ &\leq \|(L_K + \lambda I)^{-1/2}(L_K - L_{K,\mathbf{X}})(L_K + \lambda I)^{-1/2}\| \|(L_K + \lambda I)^{-1/2}\| \leq \left( \frac{\kappa^2}{3n\lambda} + \sqrt{\frac{\kappa^2}{n\lambda}} \right) \frac{1}{\sqrt{\lambda}}. \end{aligned}$$

**Lemma D.5.** For any  $0 < \delta < 1$ , with probability at least  $1 - \delta$ , we have

$$\|(L_{K,\mathbf{X}} + \lambda I)^{-1/2}(L_K + \lambda I)^{1/2}\| \leq 1 + \frac{2\kappa}{\sqrt{n\lambda}} \left\{ \frac{\kappa}{\sqrt{n\lambda}} + \sqrt{\mathcal{N}(\lambda)} \right\} \log \left( \frac{2}{\delta} \right).$$

**Proof** [Proof of Lemma D.5] By virtue of a second order decomposition of operator difference in Lemma 16 [LGZ17], we have

$$A^{-1} - B^{-1} = B^{-1}(B - A)A^{-1}(B - A)B^{-1} + B^{-1}(B - A)B^{-1},$$

which leads to

$$A^{-1}B = I + B^{-1}(B - A) + B^{-1}(B - A)A^{-1}(B - A). \quad (\text{D.1})$$

Accordingly, denote  $A := L_{K,\mathbf{X}} + \lambda I$  and  $B := L_K + \lambda I$ , we can derive that

$$\begin{aligned} \|(L_{K,\mathbf{X}} + \lambda I)^{-1/2}(L_K + \lambda I)^{1/2}\| &\leq \|(L_{K,\mathbf{X}} + \lambda I)^{-1}(L_K + \lambda I)\|^{1/2} \\ &\leq \sqrt{1 + \lambda^{-1/2}\|(L_K + \lambda I)^{-1/2}(L_K - L_{K,\mathbf{X}})\| + \lambda^{-1}\|(L_K + \lambda I)^{-1/2}(L_K - L_{K,\mathbf{X}})\|^2} \\ &\leq \sqrt{1 + \mathcal{A} + \mathcal{A}^2} \leq 1 + \mathcal{A}, \end{aligned}$$

where  $\mathcal{A} := \frac{2\kappa}{\sqrt{n\lambda}} \left\{ \frac{\kappa}{\sqrt{n\lambda}} + \sqrt{\mathcal{N}(\lambda)} \right\} \log(2/\delta)$  by Lemma D.2. The first inequality holds by  $\|A^s B^s\| \leq \|AB\|^s$  with  $0 \leq s \leq 1$  for positive operators  $A$  and  $B$  on Hilbert spaces [BK10]. The second inequality can be derived by Eq. (D.1),  $\|(L_{K,\mathbf{X}} + \lambda I)^{-1}\| \leq 1/\lambda$  and  $\|(L_K + \lambda I)^{-1/2}\| \leq 1/\sqrt{\lambda}$ .  $\square$

**Remark:** Lemma 7.2 in [RCR13] gives  $\|(L_{K,\mathbf{X}} + \lambda I)^{-1/2}(L_K + \lambda I)^{1/2}\| \leq \sqrt{2}$  by assuming  $\lambda > \frac{9}{n} \log \frac{2}{\delta}$ ; whereas our result does not require extra conditions on  $\lambda$ .

Based on the above lemmas, we are ready to prove Theorem 3. **Proof** [Proof of Theorem 3] We first estimate  $\|(L_{K,\mathbf{X}} + \lambda I)^{-1/2}(L_K + \lambda I)^{1/2}\|$  in Lemma D.5 by taking  $\lambda := \bar{c}n^{-\vartheta}$  and the capacity condition in Assumption 5:  $\mathcal{N}(\lambda) \leq Q^2\lambda^{-\eta}$  with  $\eta \in [0, 1]$ . Accordingly, we have

$$\begin{aligned} \|(L_{K,\mathbf{X}} + \lambda I)^{-1/2}(L_K + \lambda I)^{1/2}\| &\leq 1 + \frac{2\kappa}{\sqrt{n\lambda}} \left\{ \frac{\kappa}{\sqrt{n\lambda}} + \sqrt{\mathcal{N}(\lambda)} \right\} \log \left( \frac{2}{\delta} \right) \\ &\leq 1 + \left( \frac{2\kappa^2}{\bar{c}} n^{-(1-\vartheta)} + 2\kappa\bar{c}^{-(\frac{1}{2}+\frac{\eta}{2})} Q n^{-\frac{1-\vartheta-\vartheta\eta}{2}} \right) \log \left( \frac{2}{\delta} \right) \\ &\leq \left( 1 + \frac{2\kappa(\kappa + Q)}{\bar{c}} n^{-\frac{1-\vartheta-\vartheta\eta}{2}} \right) \log \left( \frac{2}{\delta} \right), \end{aligned}$$

where we use  $\log^r(2/\delta) \leq \log(2/\delta)$  due to  $\log(2/\delta) > 1$  in the last inequality. Since  $\|(L_{K,\mathbf{X}} + \lambda I)^{-1/2}(L_K + \lambda I)^{1/2}\|$  converges to zero when  $n$  is large enough, we require  $\vartheta < \frac{1}{1+\eta}$  to ensure a positive convergence rate, which implies  $\vartheta \leq 1$ . Then we bound  $\|(L_K + \lambda I)^{-1/2}(L_K - L_{K,\mathbf{X}})\|^r$  by Lemma D.2. By virtue of  $(a+b)^r \leq a^r + b^r$  for any  $r \in (0, 1]$  and  $a, b \geq 0$ , we have

$$\begin{aligned} \|(L_K + \lambda I)^{-1/2}(L_K - L_{K,\mathbf{X}})\|^r &\leq \left(\frac{2\kappa}{\sqrt{n}}\right)^r \left\{ \frac{\kappa}{(n\lambda)^{\frac{r}{2}}} + [\mathcal{N}(\lambda)]^{\frac{r}{2}} \right\} \log\left(\frac{2}{\delta}\right) \\ &\leq (2\kappa)^r (n\bar{c})^{-\frac{r}{2}} \left[ \kappa n^{-\frac{r(1-\vartheta)}{2}} + \frac{Q}{\bar{c}^{\frac{\eta r}{2}}} n^{\frac{\vartheta \eta r}{2}} \right] \log\left(\frac{2}{\delta}\right) \\ &\leq \frac{2\kappa(Q + \kappa)}{\bar{c}} n^{-\frac{(1-\vartheta\eta)r}{2}} \log\left(\frac{2}{\delta}\right), \end{aligned}$$

where the second one admits by the capacity condition in Assumption 5. Similarly, to bound  $\|(L_K + \lambda I)^{-1/2}(L_K - L_{K,\mathbf{X}})(L_K + \lambda I)^{-1}\|^{1-r}$  by Lemma D.4, we can derive that

$$\begin{aligned} \|(L_K + \lambda I)^{-1/2}(L_K - L_{K,\mathbf{X}})(L_K + \lambda I)^{-1}\|^{1-r} &\leq \lambda^{-\frac{1-r}{2}} \left( \kappa^2 (n\lambda)^{-(1-r)} + \kappa (n\lambda)^{-\frac{1-r}{2}} \right) \\ &\leq \frac{\kappa^2}{\bar{c}} \left( n^{\frac{3}{2}\vartheta-1)(1-r)} + n^{(\vartheta-\frac{1}{2})(1-r)} \right) \\ &\leq \frac{\kappa^2}{\bar{c}} n^{(\vartheta-\frac{1}{2})(1-r)}. \end{aligned}$$

Combining the above three inequalities, we have

$$\begin{aligned} \|f_{\mathbf{X},\lambda} - f_\lambda\| &\leq \frac{4R\kappa^3(Q + \kappa)^2}{\bar{c}^3} n^{-\frac{(1-\vartheta\eta)r+\vartheta}{2}} n^{(\vartheta-\frac{1}{2})(1-r)} \log^2\left(\frac{2}{\delta}\right) \\ &\leq \widetilde{C_{R,Q,\kappa,\bar{c}}} n^{-\frac{1-\vartheta(\eta r+1-2r)}{2}} \log^2\left(\frac{2}{\delta}\right), \end{aligned}$$

where  $\widetilde{C_{R,Q,\kappa,\bar{c}}} := 4R\kappa^3(Q + \kappa)^2/\bar{c}^3$  is independent of  $n$  and  $d$ .

Finally, the bias can be bounded by

$$\begin{aligned} \mathbf{B} &\leq 2\|f_{\mathbf{X},\lambda} - f_\lambda\|_{\mathcal{L}_{\rho_{\mathbf{X}}}^2}^2 + 2\|f_\lambda - f_\rho\|_{\mathcal{L}_{\rho_{\mathbf{X}}}^2}^2 \\ &\leq 2R^2 n^{-2\vartheta r} + \widetilde{C}_1 n^{-[1-\vartheta(\eta r+1-2r)]} \log^4\left(\frac{2}{\delta}\right) \\ &\leq \widetilde{C} n^{-2\vartheta r} \log^4\left(\frac{2}{\delta}\right), \end{aligned}$$

where the third inequality holds by  $2\vartheta r \leq 1 - \vartheta(\eta r + 1 - 2r)$  due to  $\vartheta \leq \frac{1}{1+\eta}$ , and  $\widetilde{C}, \widetilde{C}_1$  are some constants independent of  $n$  and  $d$ . Accordingly, we can conclude the proof.  $\square$

## E Proof for the variance

Formally, we have the following theorem to bound the variance.

**Theorem 4.** (Variance) Under Assumptions 2, 3, then for  $0 < \delta < 1$  with probability  $1 - \delta - d^{-2}$ ,  $\theta = \frac{1}{2} - \frac{2}{8+m}$ , and  $d$  large enough, for any given  $\varepsilon > 0$ , we have

$$\mathbf{V} \lesssim \mathbf{V}_1 + \mathbf{V}_2,$$

where  $\mathbf{V}_1 := \frac{\sigma^2 \beta}{d} \mathcal{N}_{\widetilde{\mathbf{X}}}^{n\lambda+\gamma}$  and  $\mathbf{V}_2$  is the residual term with

$$\mathbf{V}_2 := \begin{cases} \frac{\sigma^2 \log^{2+4\varepsilon} d}{(n\lambda + \gamma)^2 d^{4\theta-1}}, & \text{inner-product kernels} \\ \frac{\sigma^2}{(n\lambda + \gamma)^2} d^{-2\theta} \log^{1+\varepsilon} d, & \text{radial kernels.} \end{cases}$$

For inner-product kernels, our proof framework follows [LR20], and is briefly discussed in Section E.1. Nevertheless, error bound on radial kernels has not been investigated in [LR20] and is more subtle to handle (than that of inner-product kernels) due to the additionally introduced  $\mathbf{A}$  and  $\mathbf{A} \odot \mathbf{A}$  in Table 2. Accordingly, we mainly focus on proofs for radial kernels.

## E.1 Inner-product kernel matrices

In this subsection, we consider the inner-product kernel case with  $k(\mathbf{x}, \mathbf{x}') = h\left(\frac{1}{d}\langle \mathbf{x}, \mathbf{x}' \rangle\right)$ . We briefly introduce our results that can be derived from proofs of Theorem 2 in [LR20] for completeness.

To prove Theorem 4, define

$$\widetilde{\mathbf{K}}^{\text{lin}}(\mathbf{X}, \mathbf{X}) := (n\lambda + \gamma)\mathbf{I} + \alpha\mathbf{1}\mathbf{1}^\top + \beta \frac{\mathbf{X}\mathbf{X}^\top}{d} \in \mathbb{R}^{n \times n}, \quad k^{\text{lin}}(\mathbf{x}, \mathbf{X}) := h(0)\mathbf{1} + \beta \frac{\mathbf{X}\mathbf{x}^\top}{d} \in \mathbb{R}^{n \times 1}, \quad (\text{E.1})$$

and  $k^{\text{lin}}(\mathbf{X}, \mathbf{x})$  is the transpose of  $k^{\text{lin}}(\mathbf{x}, \mathbf{X})$ . Note that  $\gamma$  in  $\widetilde{\mathbf{K}}^{\text{lin}}$  corresponds to the *implicit* regularization and  $n\lambda$  corresponds to the *explicit* regularization. Now we prove Theorem 4 for inner-product kernels.

**Proof** [Proof of Theorem 4 for inner-product kernels] According to the definition of  $\mathbf{v}$ , we have

$$\begin{aligned} \mathbf{v} &= \mathbb{E}_{\mathbf{x}, y} \text{tr} \left[ k(\mathbf{x}, \mathbf{X})^\top (\mathbf{K} + n\lambda\mathbf{I})^{-1} \boldsymbol{\epsilon} \boldsymbol{\epsilon}^\top (\mathbf{K} + n\lambda\mathbf{I})^{-1} k(\mathbf{x}, \mathbf{X}) \right] = \mathbb{E}_{\mathbf{x}} \left\| (\mathbf{K} + n\lambda\mathbf{I})^{-1} k(\mathbf{x}, \mathbf{X}) \right\|_2^2 \mathbb{E}_{y|\mathbf{x}} \|\boldsymbol{\epsilon}\|_2^2 \\ &\leq \sigma^2 \mathbb{E}_{\mathbf{x}} \left\| (\mathbf{K} + n\lambda\mathbf{I})^{-1} k(\mathbf{x}, \mathbf{X}) \right\|_2^2 \\ &\leq \sigma^2 \left\| (\mathbf{K} + n\lambda\mathbf{I})^{-1} \widetilde{\mathbf{K}}^{\text{lin}} \right\|_2^2 \mathbb{E}_{\mathbf{x}} \left\| [\widetilde{\mathbf{K}}^{\text{lin}}]^{-1} k^{\text{lin}}(\mathbf{x}, \mathbf{X}) \right\|_2^2 + \sigma^2 \left\| (\mathbf{K} + n\lambda\mathbf{I})^{-1} \right\|_2^2 \mathbb{E}_{\mathbf{x}} \left\| k(\mathbf{x}, \mathbf{X}) - k^{\text{lin}}(\mathbf{x}, \mathbf{X}) \right\|_2^2, \end{aligned} \quad (\text{E.2})$$

where the first inequality comes from Assumption 2. To bound the terms in Eq. (E.2), we need

$$\begin{aligned} \mathbb{E}_{\mathbf{x}} \left\| [\widetilde{\mathbf{K}}^{\text{lin}}]^{-1} k^{\text{lin}}(\mathbf{x}, \mathbf{X}) \right\|_2^2 &= \mathbb{E}_{\mathbf{x}} \text{tr} \left[ \left[ \widetilde{\mathbf{K}}^{\text{lin}} \right]^{-1} \left( \beta \frac{\mathbf{X}\mathbf{x}}{d} + h(0)\mathbf{1} \right) \left( \beta \frac{\mathbf{x}^\top \mathbf{X}^\top}{d} + h(0)\mathbf{1}^\top \right) \left[ \widetilde{\mathbf{K}}^{\text{lin}} \right]^{-1} \right] \\ &\leq \frac{1}{d} \|\boldsymbol{\Sigma}_d\|_2 \text{tr} \left( \left[ \widetilde{\mathbf{K}}^{\text{lin}} \right]^{-1} \beta^2 \frac{\mathbf{X}\mathbf{X}^\top}{d} \left[ \widetilde{\mathbf{K}}^{\text{lin}} \right]^{-1} \right) + \frac{1}{d} \text{tr} \left( \left[ \widetilde{\mathbf{K}}^{\text{lin}} \right]^{-1} h(0)^2 \mathbf{1}\mathbf{1}^\top \left[ \widetilde{\mathbf{K}}^{\text{lin}} \right]^{-1} \right) \\ &\leq \frac{\beta}{d} \|\boldsymbol{\Sigma}_d\|_2 \sum_{j=1}^n \frac{\lambda_j(\widetilde{\mathbf{X}})}{\left[ n\lambda + \gamma + \lambda_j(\widetilde{\mathbf{X}}) \right]^2} + \frac{1}{d} \frac{h(0)^2 n}{\left[ n\lambda + \gamma + \lambda_1(\widetilde{\mathbf{X}}) \right]^2} \\ &\asymp \frac{\beta}{d} \mathcal{N}_{\widetilde{\mathbf{X}}}^{n\lambda + \gamma} + \mathcal{O}\left(\frac{1}{nd}\right). \end{aligned} \quad (\text{E.3})$$

To bound the remaining terms in Eq. (E.2), we also need the following results that can be obtained from [LR20]:

(i) By Proposition A.2 in [LR20], with probability at least  $1 - \delta - d^{-2}$ , for  $\theta = \frac{1}{2} - \frac{2}{8+m}$  and any given  $\varepsilon > 0$ , we have

$$\left\| \mathbf{K} + n\lambda\mathbf{I} - \widetilde{\mathbf{K}}^{\text{lin}} \right\|_2 \leq d^{-\theta} (\delta^{-1/2} + \log^{0.5+\varepsilon} d) \quad \text{and} \quad \mathbb{E}_{\mathbf{x}} \left\| k(\mathbf{x}, \mathbf{X}) - k^{\text{lin}}(\mathbf{x}, \mathbf{X}) \right\|_2^2 \leq \widetilde{C}_1 d^{-(4\theta-1)} \log^{2+4\varepsilon} d.$$

(ii)  $\left\| (\mathbf{K} + n\lambda\mathbf{I})^{-1} \right\|_2 \leq \frac{2}{n\lambda + \gamma}$  and  $\left\| (\mathbf{K} + n\lambda\mathbf{I})^{-1} \widetilde{\mathbf{K}}^{\text{lin}} \right\|_2 \leq 2$  provided  $d$  is large enough such that  $d^{-\theta} (\delta^{-1/2} + \log^{0.5+\varepsilon} d) \leq \gamma/2$ .

Combining the above results, with probability at least  $1 - \delta - d^{-2}$ , for any given  $\varepsilon > 0$ , The error bound for the variance in Eq. (E.2) can be further given by

$$\begin{aligned} \mathbf{v} &\leq \sigma^2 \mathbb{E}_{\mathbf{x}} \left\| (\mathbf{K} + n\lambda\mathbf{I})^{-1} k(\mathbf{x}, \mathbf{X}) \right\|_2^2 \\ &\leq 2\sigma^2 \left\| (\mathbf{K} + n\lambda\mathbf{I})^{-1} \widetilde{\mathbf{K}}^{\text{lin}} \right\|_2^2 \mathbb{E}_{\mathbf{x}} \left\| [\widetilde{\mathbf{K}}^{\text{lin}}]^{-1} k^{\text{lin}}(\mathbf{x}, \mathbf{X}) \right\|_2^2 + 2\sigma^2 \left\| \mathbf{K}^{-1} \right\|_2^2 \mathbb{E}_{\mathbf{x}} \left\| k(\mathbf{x}, \mathbf{X}) - k^{\text{lin}}(\mathbf{x}, \mathbf{X}) \right\|_2^2 \\ &\asymp \frac{8\sigma^2\beta}{d} \|\boldsymbol{\Sigma}_d\|_2 \sum_{j=1}^n \frac{\lambda_j(\widetilde{\mathbf{X}})}{\left[ n\lambda + \gamma + \lambda_j(\widetilde{\mathbf{X}}) \right]^2} + \frac{8\sigma^2}{(n\lambda + \gamma)^2} \widetilde{C}_1 d^{-(4\theta-1)} \log^{2+4\varepsilon} d \\ &\asymp \frac{\sigma^2\beta}{d} \mathcal{N}_{\widetilde{\mathbf{X}}}^{n\lambda + \gamma} + \frac{\sigma^2}{(n\lambda + \gamma)^2} d^{-(4\theta-1)} \log^{2+4\varepsilon} d, \end{aligned}$$

which concludes the proof.  $\square$

## E.2 Radial kernel matrices

In this subsection, we consider the radial kernel case with  $k(\mathbf{x}, \mathbf{x}') = h\left(\frac{1}{d}\|\mathbf{x} - \mathbf{x}'\|_2^2\right)$ . Since the linearization of radial kernel matrices incurs in two additional terms  $\mathbf{A}$  and  $\mathbf{A} \odot \mathbf{A}$ , estimation for radial kernels is more technical than that of inner-product kernels. Accordingly, to prove Theorem 4 for radial kernels, we need to introduce the following notations and auxiliary results.

### E.2.1 Auxiliary results

Recall  $\tau := \text{tr}(\boldsymbol{\Sigma}_d)/d$ , define

$$\begin{aligned} \widetilde{\mathbf{K}}^{\text{lin}}(\mathbf{X}, \mathbf{X}) &:= (\gamma + n\lambda)\mathbf{I} + \alpha\mathbf{1}\mathbf{1}^\top + \beta\frac{\mathbf{X}\mathbf{X}^\top}{d} + h'(2\tau)\mathbf{A} + \frac{1}{2}h''(2\tau)\mathbf{A} \odot \mathbf{A} \\ k^{\text{lin}}(\mathbf{x}, \mathbf{X}) &:= h(2\tau)\mathbf{1} + \beta\frac{\mathbf{X}\mathbf{x}^\top}{d} - \frac{\beta}{2}\mathbf{A}(\mathbf{x}, \mathbf{X}) \in \mathbb{R}^{n \times 1}, \end{aligned} \quad (\text{E.4})$$

where  $\mathbf{A}(\mathbf{x}, \mathbf{X}) := \psi_{\mathbf{x}} + [\psi_1, \psi_2, \dots, \psi_n]^\top$  with  $\psi_{\mathbf{x}} = \|\mathbf{x}\|_2^2/d - \tau$  and  $\psi_i = \|\mathbf{x}_i\|_2^2/d - \tau$  for  $i = 1, 2, \dots, n$ . As discussed in Appendix B, we conclude that  $\widetilde{\mathbf{K}}^{\text{lin}}$  admits the same eigenvalue decay as  $\widetilde{\mathbf{X}}$  since  $\mathbf{A}$  is a rank-2 matrix. Accordingly, we have the following results.

**Proposition E.1.** *Given  $\mathbf{A}(\mathbf{x}, \mathbf{X})$  in Eq. (E.4), we have  $\mathbb{E}_{\mathbf{x}}[\mathbf{X}\mathbf{x}\mathbf{A}(\mathbf{X}, \mathbf{x})] = \mu_3\mathbf{X}\boldsymbol{\Sigma}_d^{1/2}\text{diag}(\boldsymbol{\Sigma}_d)\mathbf{1}_n^\top$ , where  $\mu_3 := \mathbb{E}[\mathbf{t}(j)^3]$  does not depend on  $j$  because each entry in  $\mathbf{t}$  are independent for  $j = 1, 2, \dots, d$ . Further,  $\mathbb{E}_{\mathbf{x}}[\mathbf{X}\mathbf{x}\mathbf{A}(\mathbf{X}, \mathbf{x})]$  is a rank-one matrix with its eigenvalue  $\lambda_1(\mathbb{E}_{\mathbf{x}}[\mathbf{X}\mathbf{x}\mathbf{A}(\mathbf{X}, \mathbf{x})]) = \mathcal{O}(\sqrt{n/d})$ .*

**Proof** [Proof of Proposition E.1] According to the definition in Assumption 3,  $\mathbf{x}_i = \boldsymbol{\Sigma}_d^{1/2}\mathbf{t}_i$  with  $\mathbb{E}[\mathbf{t}_i(j)] = 0$  and  $\mathbb{V}[\mathbf{t}_i(j)] = 1$ , we have the following expression

$$\mathbb{E}_{\mathbf{t}}[\mathbf{t}\mathbf{t}^\top\boldsymbol{\Sigma}_d\mathbf{t}] = \mathbb{E}_{\mathbf{t}}\left[\mathbf{t}\sum_{i,j=1}^d \mathbf{t}(i)(\boldsymbol{\Sigma}_d)_{ij}\mathbf{t}(j)\right] = \mu_3[(\boldsymbol{\Sigma}_d)_{11}, (\boldsymbol{\Sigma}_d)_{22}, \dots, (\boldsymbol{\Sigma}_d)_{dd}]^\top,$$

where  $\mu_3 := \mathbb{E}(\mathbf{t}_i^3)$ . Accordingly,  $\mathbb{E}_{\mathbf{x}}[\mathbf{X}\mathbf{x}\mathbf{A}(\mathbf{X}, \mathbf{x})]$  can be computed by

$$\begin{aligned} \mathbb{E}_{\mathbf{x}}[\mathbf{X}\mathbf{x}\mathbf{A}(\mathbf{X}, \mathbf{x})] &= \mathbb{E}_{\mathbf{x}}[\mathbf{X}\mathbf{x}(\psi_1 + \psi_{\mathbf{x}}), \mathbf{X}\mathbf{x}(\psi_2 + \psi_{\mathbf{x}}), \dots, \mathbf{X}\mathbf{x}(\psi_n + \psi_{\mathbf{x}})] \\ &= \mathbb{E}_{\mathbf{x}}[\mathbf{X}\mathbf{x}\psi_{\mathbf{x}}, \mathbf{X}\mathbf{x}\psi_{\mathbf{x}}, \dots, \mathbf{X}\mathbf{x}\psi_{\mathbf{x}}] \\ &= \mathbf{X}\boldsymbol{\Sigma}_d^{1/2}\left[\frac{\mathbb{E}_{\mathbf{t}}[\mathbf{t}\mathbf{t}^\top\boldsymbol{\Sigma}_d\mathbf{t}]}{d}, \frac{\mathbb{E}_{\mathbf{t}}[\mathbf{t}\mathbf{t}^\top\boldsymbol{\Sigma}_d\mathbf{t}]}{d}, \dots, \frac{\mathbb{E}_{\mathbf{t}}[\mathbf{t}\mathbf{t}^\top\boldsymbol{\Sigma}_d\mathbf{t}]}{d}\right] \\ &= \mu_3\mathbf{X}\boldsymbol{\Sigma}_d^{1/2}\text{diag}(\boldsymbol{\Sigma}_d)\mathbf{1}_n^\top. \end{aligned}$$

Note that, the matrix  $\text{diag}(\boldsymbol{\Sigma}_d)\mathbf{1}_n^\top$  is a rank-one matrix, which implies  $\text{rank}(\mathbf{X}\boldsymbol{\Sigma}_d^{1/2}\text{diag}(\boldsymbol{\Sigma}_d)\mathbf{1}_n^\top) \leq 1$ . Accordingly, its non-zero eigenvalue  $\lambda_1(\mathbf{X}\boldsymbol{\Sigma}_d^{1/2}\text{diag}(\boldsymbol{\Sigma}_d)\mathbf{1}_n^\top)$  admits

$$\frac{1}{d}\lambda_1(\mathbf{X}\boldsymbol{\Sigma}_d^{1/2}\text{diag}(\boldsymbol{\Sigma}_d)\mathbf{1}_n^\top) = \frac{1}{d}\sum_{i=1}^n \mathbf{x}_i^\top \boldsymbol{\Sigma}_d^{\frac{1}{2}} \text{diag}(\boldsymbol{\Sigma}_d) = \frac{1}{d}\sum_{i=1}^n \mathbf{t}_i^\top \boldsymbol{\Sigma}_d \text{diag}(\boldsymbol{\Sigma}_d).$$

Due to  $\mathbb{E}[\mathbf{t}_i^\top \boldsymbol{\Sigma}_d \text{diag}(\boldsymbol{\Sigma}_d)] = 0$  and  $\mathbb{V}[\mathbf{t}_i^\top \boldsymbol{\Sigma}_d \text{diag}(\boldsymbol{\Sigma}_d)] = \|\boldsymbol{\Sigma}_d \text{diag}(\boldsymbol{\Sigma}_d)\|_2^2$ , which, with a central limit theorem argument, implies  $\sum_{i=1}^n \mathbf{t}_i^\top \boldsymbol{\Sigma}_d \text{diag}(\boldsymbol{\Sigma}_d) = \mathcal{O}(\sqrt{nd})$  due to  $\|\boldsymbol{\Sigma}_d \text{diag}(\boldsymbol{\Sigma}_d)\|_2 \leq \|\boldsymbol{\Sigma}_d\|_2 \|\text{diag}(\boldsymbol{\Sigma}_d)\|_2 \leq \widetilde{C}\|\text{diag}(\boldsymbol{\Sigma}_d)\|_2$ . Accordingly, we can conclude that  $\frac{1}{d}\lambda_1(\mathbf{X}\boldsymbol{\Sigma}_d^{1/2}\text{diag}(\boldsymbol{\Sigma}_d)\mathbf{1}_n^\top) = \mathcal{O}(\sqrt{n/d})$ .  $\square$

**Proposition E.2.** *Given  $\mathbf{A}(\mathbf{x}, \mathbf{X})$  in Eq. (E.4), we have  $\mathbb{E}_{\mathbf{x}}[\mathbf{A}(\mathbf{x}, \mathbf{X})\mathbf{A}(\mathbf{X}, \mathbf{x})] = \psi\psi^\top + \mathcal{O}(1/d)$ . Further, it has only one non-zero eigenvalue that admits  $\lambda_1(\mathbb{E}_{\mathbf{x}}[\mathbf{A}(\mathbf{x}, \mathbf{X})\mathbf{A}(\mathbf{X}, \mathbf{x})]) = \mathcal{O}(n)$ .*

**Proof** [Proof of Proposition E.2] By virtue of the following results [EK10]

$$\begin{aligned}\frac{1}{d}\mathbb{E}_{\mathbf{x}}\|\mathbf{x}\|_2^2 &= \frac{1}{d}\mathbb{E}_{\mathbf{t}}[\mathbf{t}^\top \boldsymbol{\Sigma}_d \mathbf{t}] = \tau \\ \mathbb{V}_{\mathbf{x}}\left[\frac{\|\mathbf{x}\|_2^2}{d}\right] &= \frac{1}{d^2}\left((\mu_4 - 3)\sum_{i=1}^d((\boldsymbol{\Sigma}_d)_{ii})^2 + 2\text{tr}(\boldsymbol{\Sigma}_d^2)\right) = \mathcal{O}\left(\frac{1}{d}\right),\end{aligned}$$

where  $\mu_4 := \mathbb{E}[\mathbf{t}(i)^4]$  does not depend on  $i$ . Accordingly, each entry in  $\mathbb{E}_{\mathbf{x}}[\mathbf{A}(\mathbf{x}, \mathbf{X})\mathbf{A}(\mathbf{X}, \mathbf{x})]$  can be computed as

$$\begin{aligned}\mathbb{E}_{\mathbf{x}}[\mathbf{A}(\mathbf{x}, \mathbf{X})\mathbf{A}(\mathbf{X}, \mathbf{x})]_{ij} &= \mathbb{E}_{\mathbf{x}}[(\psi_i + \psi_{\mathbf{x}})(\psi_j + \psi_{\mathbf{x}})] \\ &= \psi_i\psi_j + (\psi_i + \psi_j)\mathbb{E}_{\mathbf{x}}\psi_{\mathbf{x}} + \mathbb{E}_{\mathbf{x}}[\psi_{\mathbf{x}}^2] \\ &= \psi_i\psi_j + \mathbb{V}_{\mathbf{x}}\left[\frac{\|\mathbf{x}\|_2^2}{d}\right] \\ &= \psi_i\psi_j + \frac{\mu_4 - 3}{d^2}\text{tr}(\boldsymbol{\Sigma}_d \odot \boldsymbol{\Sigma}_d) + \frac{2\text{tr}(\boldsymbol{\Sigma}_d^2)}{d^2}.\end{aligned}$$

Then we have

$$\mathbb{E}_{\mathbf{x}}[\mathbf{A}(\mathbf{x}, \mathbf{X})\mathbf{A}(\mathbf{X}, \mathbf{x})] = \boldsymbol{\psi}\boldsymbol{\psi}^\top + \mathcal{O}(1/d).$$

Therefore,  $\boldsymbol{\psi}\boldsymbol{\psi}^\top$  is a rank-one matrix with  $\lambda_1(\boldsymbol{\psi}\boldsymbol{\psi}^\top) = \|\boldsymbol{\psi}\|_2^2 = \mathcal{O}(n)$ . Then  $\lambda_1(\mathbb{E}_{\mathbf{x}}[\mathbf{A}(\mathbf{x}, \mathbf{X})\mathbf{A}(\mathbf{X}, \mathbf{x})])$  can be estimated by

$$\|\boldsymbol{\psi}\|_2^2 \leq \lambda_1(\mathbb{E}_{\mathbf{x}}[\mathbf{A}(\mathbf{x}, \mathbf{X})\mathbf{A}(\mathbf{X}, \mathbf{x})]) \leq \|\boldsymbol{\psi}\|_2^2 + n \underbrace{\left[\frac{\mu_4 - 3}{d^2}\text{tr}(\boldsymbol{\Sigma}_d \odot \boldsymbol{\Sigma}_d) + \frac{2\text{tr}(\boldsymbol{\Sigma}_d^2)}{d^2}\right]}_{=\mathcal{O}(1/d)},$$

which implies  $\lambda_1(\mathbb{E}_{\mathbf{x}}[\mathbf{A}(\mathbf{x}, \mathbf{X})\mathbf{A}(\mathbf{X}, \mathbf{x})]) = \mathcal{O}(n)$ . □

**Lemma E.3.** *Given a radial kernel, under Assumption 3, for  $\theta = \frac{1}{2} - \frac{2}{8+m}$ , we have with probability at least  $1 - d^{-2}$  with respect to the draw of  $\mathbf{X}$ , for  $d$  large enough, for any given  $\varepsilon > 0$ , we have*

$$\mathbb{E}_{\mathbf{x}}\|k(\mathbf{x}, \mathbf{X}) - k^{\text{lin}}(\mathbf{x}, \mathbf{X})\|_2^2 \leq \widetilde{C}_1 d^{-2\theta} \log^{1+\varepsilon} d,$$

where  $\widetilde{C}_1$  is some constant independent of  $n$  and  $d$ .

**Remark:** In fact, we only need the  $(5 + m)$ -moment in Assumption 3 but we still follow with it for simplicity. **Proof** [Proof of Lemma E.3] We start with the entry-wise Taylor expansion for the smooth kernel at  $2\tau$  with  $\tau := \text{tr}(\boldsymbol{\Sigma}_d)/d$

$$\begin{aligned}k(\mathbf{x}, \mathbf{x}_j) &= h\left(\frac{1}{d}\|\mathbf{x} - \mathbf{x}_j\|_2^2\right) = h(2\tau) + h'(2\tau)\left(\frac{1}{d}\|\mathbf{x} - \mathbf{x}_j\|_2^2 - 2\tau\right) + \frac{h''(2\tau)}{2}\left(\frac{1}{d}\|\mathbf{x} - \mathbf{x}_j\|_2^2 - 2\tau\right)^2 + \mathcal{O}(d^{-3/2}) \\ &= h(2\tau) + h'(2\tau)\left(\psi_{\mathbf{x}} + \psi_j - \frac{2\mathbf{x}^\top \mathbf{x}_j}{d}\right) + \frac{h''(2\tau)}{2}\left(\psi_{\mathbf{x}} + \psi_j - \frac{2\mathbf{x}^\top \mathbf{x}_j}{d}\right)^2 + \mathcal{O}(d^{-3/2}),\end{aligned}$$

where  $\psi_j = \|\mathbf{x}_j\|_2^2/d - \tau$  for  $j = 1, 2, \dots, n$  as defined before. Accordingly, by virtue of  $k^{\text{lin}}(\mathbf{x}, \mathbf{x}_j) = \frac{\beta \mathbf{x}^\top \mathbf{x}_j}{d} - \frac{\beta}{2}(\psi_{\mathbf{x}} + \psi_j)$  and Corollary 2 in [EK10], with probability at least  $1 - d^{-2}$ , for any  $\varepsilon > 0$ , we have

$$k(\mathbf{x}, \mathbf{x}_j) - k^{\text{lin}}(\mathbf{x}, \mathbf{x}_j) = \frac{h''(2\tau)}{2}\left(\frac{1}{d}\|\mathbf{x} - \mathbf{x}_j\|_2^2 - 2\tau\right)^2 \leq \widetilde{C} d^{-1+\frac{4}{m}} (\log d)^{\frac{1+\varepsilon}{2}},$$

where we only need  $(5 + m)$ -moment. Therefore, with probability at least  $1 - d^{-2}$ , for any given  $\varepsilon > 0$ , we have

$$\|k(\mathbf{x}, \mathbf{X}) - k^{\text{lin}}(\mathbf{x}, \mathbf{X})\|_2 \leq C_1 d^{-1/2+\frac{4}{m}} (\log d)^{\frac{1+\varepsilon}{2}} \leq \widetilde{C}_1 d^{-\theta} (\log d)^{\frac{1+\varepsilon}{2}},$$



which implies

$$\mathbb{E}_{\mathbf{x}} \|k(\mathbf{x}, \mathbf{X}) - k^{\text{lin}}(\mathbf{x}, \mathbf{X})\|_2^2 \leq \widetilde{C}_2 d^{-2\theta} \log^{1+\varepsilon} d,$$

where  $\widetilde{C}_1$  and  $\widetilde{C}_2$  are some constant independent of  $n$  and  $d$ .  $\square$

## E.2.2 Proofs of Theorem 4 for radial kernels

Now we are ready to prove Theorem 4 for radial kernels. **Proof** [Proof of Theorem 4 for radial kernels] Similar to Eq. (E.2), to estimate  $\mathbf{v} \leq \sigma^2 \mathbb{E}_{\mathbf{x}} \|(\mathbf{K} + n\lambda \mathbf{I})^{-1} k(\mathbf{x}, \mathbf{X})\|_2^2$ , we need to bound subsequently the following terms:  $\|\mathbf{K} + n\lambda \mathbf{I} - \widetilde{\mathbf{K}}^{\text{lin}}(\mathbf{X}, \mathbf{X})\|_2$ ,  $\|(\mathbf{K} + n\lambda \mathbf{I})^{-1}\|_2$ ,  $\|(\mathbf{K} + n\lambda \mathbf{I})^{-1} \widetilde{\mathbf{K}}^{\text{lin}}(\mathbf{X}, \mathbf{X})\|_2$ ,  $\mathbb{E}_{\mathbf{x}} \|[\widetilde{\mathbf{K}}^{\text{lin}}(\mathbf{X}, \mathbf{X})]^{-1} k^{\text{lin}}(\mathbf{x}, \mathbf{X})\|_2^2$ , and  $\mathbb{E}_{\mathbf{x}} \|k(\mathbf{x}, \mathbf{X}) - k^{\text{lin}}(\mathbf{x}, \mathbf{X})\|_2^2$ .

In [EK10], the approximation error between radial kernel matrices and their linearization can be decomposed into three parts: the first-order term  $A_1$ , the second-order term  $A_2$ , and the third-order term  $A_3$

$$\|\mathbf{K} + n\lambda \mathbf{I} - \widetilde{\mathbf{K}}^{\text{lin}}(\mathbf{X}, \mathbf{X})\|_2 := A_1 + A_2 + A_3,$$

where  $A_1$  and  $A_3$  admit  $\|A_1\|_2 \leq d^{-\theta} \log^{2+4\varepsilon} d$  and  $\|A_3\|_2 \leq d^{-\theta} \log^{2+4\varepsilon} d$ . The second-order term  $A_2$  admits  $\Pr(\|A_2\|_2 \leq d^{-\theta} \delta^{-1/2}) \leq \delta$  by Proposition A.2 in [LR20] and [EK10]. Accordingly, with probability at least  $1 - \delta - d^{-2}$ , for  $\theta = \frac{1}{2} - \frac{2}{8+m}$  and any given  $\varepsilon > 0$ , we have

$$\|\mathbf{K} + n\lambda \mathbf{I} - \widetilde{\mathbf{K}}^{\text{lin}}(\mathbf{X}, \mathbf{X})\|_2 \leq d^{-\theta} \left( \delta^{-1/2} + \log^{2+4\varepsilon} d \right).$$

According to Proposition E.1 and E.2, we have

$$\begin{aligned} & \mathbb{E}_{\mathbf{x}} \|[\widetilde{\mathbf{K}}^{\text{lin}}(\mathbf{X}, \mathbf{X})]^{-1} k^{\text{lin}}(\mathbf{X}, \mathbf{x})\|_2^2 \\ &= \beta^2 \mathbb{E}_{\mathbf{x}} \text{tr} \left[ [\widetilde{\mathbf{K}}^{\text{lin}}]^{-1} \left( \frac{\mathbf{X} \mathbf{x} \mathbf{x}^{\top} \mathbf{X}^{\top}}{d^2} - \frac{\mathbf{X} \mathbf{x} \mathbf{A}(\mathbf{X}, \mathbf{x})}{d} + \frac{1}{4} \mathbf{A}(\mathbf{x}, \mathbf{X}) \mathbf{A}(\mathbf{X}, \mathbf{x}) + h(2\tau)^2 \mathbf{1} \mathbf{1}^{\top} \right) [\widetilde{\mathbf{K}}^{\text{lin}}]^{-1} \right] \\ &\leq \beta^2 \text{tr} \left( [\widetilde{\mathbf{K}}^{\text{lin}}]^{-1} \left( \frac{\mathbf{X} \mathbf{X}^{\top} \|\Sigma_d\|_2}{d^2} - \frac{\mu_3 \mathbf{X} \Sigma_d^{1/2} \text{diag}(\Sigma_d) \mathbf{1}_n^{\top}}{d} + \frac{1}{4} \mathbf{A}(\mathbf{x}, \mathbf{X}) \mathbf{A}(\mathbf{X}, \mathbf{x}) + h(2\tau)^2 \mathbf{1} \mathbf{1}^{\top} \right) [\widetilde{\mathbf{K}}^{\text{lin}}]^{-1} \right) \\ &= \frac{\beta^2 \|\Sigma_d\|_2}{d} \sum_{i=1}^n \frac{\lambda_i(\mathbf{X} \mathbf{X}^{\top} / d)}{[\lambda_i(\widetilde{\mathbf{K}}^{\text{lin}})]^2} - \frac{\beta^2 \mu_3 \lambda_1(\mathbf{X} \Sigma_d^{1/2} \text{diag}(\Sigma_d) \mathbf{1}_n^{\top})}{d [\lambda_1(\widetilde{\mathbf{K}}^{\text{lin}})]^2} + \frac{\beta^2 4\lambda_1(\mathbb{E}_{\mathbf{x}}[\mathbf{A}(\mathbf{x}, \mathbf{X}) \mathbf{A}(\mathbf{X}, \mathbf{x})]) + h(2\tau)^2 n}{[\lambda_1(\widetilde{\mathbf{K}}^{\text{lin}})]^2} \\ &\asymp \frac{\beta^2 \|\Sigma_d\|_2}{d} \sum_{i=1}^n \frac{\lambda_i(\mathbf{X} \mathbf{X}^{\top} / d)}{[\lambda_1(\widetilde{\mathbf{K}}^{\text{lin}})]^2} + \frac{\mathcal{O}(\sqrt{n/d})}{[\lambda_1(\widetilde{\mathbf{K}}^{\text{lin}})]^2} + \frac{\mathcal{O}(n)}{[\lambda_1(\widetilde{\mathbf{K}}^{\text{lin}})]^2} + \frac{\mathcal{O}(n)}{[\lambda_1(\widetilde{\mathbf{K}}^{\text{lin}})]^2} \\ &\asymp \frac{\beta}{d} \mathcal{N}_{\bar{\mathbf{X}}}^{n\lambda+\gamma} + \mathcal{O}\left(\frac{1}{n}\right). \end{aligned} \tag{E.5}$$

It can be found that, the above error bounds are the same as that of inner-product kernels, except two additional terms due to the considered  $\mathbf{A}$  and  $\mathbf{A} \odot \mathbf{A}$  in the linearization, which can be shown small in the large  $n, d$  regime.

By virtue of  $\|(\mathbf{K} + n\lambda \mathbf{I})^{-1}\|_2 \leq \frac{2}{n\lambda+\gamma}$  and  $\|(\mathbf{K} + n\lambda \mathbf{I})^{-1} \widetilde{\mathbf{K}}^{\text{lin}}\|_2 \leq 2$  in [LR20], Lemma E.3, and the above equations, with probability at least  $1 - \delta - d^{-2}$ , for any given  $\varepsilon > 0$ , we have

$$\begin{aligned} \mathbf{v} &\leq \sigma^2 \mathbb{E}_{\mathbf{x}} \|(\mathbf{K} + n\lambda \mathbf{I})^{-1} k(\mathbf{x}, \mathbf{X})\|_2^2 \\ &\leq 2\sigma^2 \left\| (\mathbf{K} + n\lambda \mathbf{I})^{-1} \widetilde{\mathbf{K}}^{\text{lin}} \right\|_2^2 \mathbb{E}_{\mathbf{x}} \|[\widetilde{\mathbf{K}}^{\text{lin}}]^{-1} k^{\text{lin}}(\mathbf{X}, \mathbf{x})\|_2^2 + 2\sigma^2 \|\mathbf{K}^{-1}\|_2^2 \mathbb{E}_{\mathbf{x}} \|k(\mathbf{x}, \mathbf{X}) - k^{\text{lin}}(\mathbf{x}, \mathbf{X})\|_2^2 \\ &\leq 8\sigma^2 \mathbb{E}_{\mathbf{x}} \|[\widetilde{\mathbf{K}}^{\text{lin}}]^{-1} k^{\text{lin}}(\mathbf{X}, \mathbf{x})\|_2^2 + \frac{8\sigma^2}{(n\lambda + \gamma)^2} \widetilde{C}_1 d^{-2\theta} \log^{1+\varepsilon} d \\ &\asymp \frac{\sigma^2 \beta}{d} \mathcal{N}_{\bar{\mathbf{X}}}^{n\lambda+\gamma} + \frac{\sigma^2}{(n\lambda + \gamma)^2} d^{-2\theta} \log^{1+\varepsilon} d, \end{aligned} \tag{E.6}$$

where the second inequality admits by Lemma E.3, and the last inequality follows by Eq. (E.5). Finally, we conclude the proof.  $\square$

## F Proof of Proposition 4.1

In this section, we discuss  $\mathcal{N}_{\widetilde{\mathbf{X}}}^{n\lambda+\gamma}$  based on three eigenvalue decays: *harmonic decay*, *polynomial decay*, and *exponential decay* under two regimes  $n < d$  and  $n > d$ .

### F.1 $n < d$ case

Recall  $b := n\lambda + \gamma > 0$ , and  $\mathcal{N}_{\widetilde{\mathbf{X}}}^b := \sum_{i=1}^n \frac{\lambda_i(\widetilde{\mathbf{X}})}{[b + \lambda_i(\widetilde{\mathbf{X}})]^2}$ , define  $F(\lambda_i) := \frac{\lambda_i}{(b + \lambda_i)^2}$  where  $\lambda_i$  is short for  $\lambda_i(\widetilde{\mathbf{X}})$ . We notice that, when  $\lambda_i \leq b$ ,  $F(\lambda_i)$  is an increasing function of  $\lambda_i$ , and thus a decreasing function of  $i$  when the above three eigenvalue decays are considered. Likewise, when  $\lambda_i \geq b$ ,  $F(\lambda_i)$  is a decreasing function of  $\lambda_i$ , and thus an increasing function of  $i$ . Without loss of generality, we assume that the first  $q$  eigenvalues satisfy  $\lambda_i \geq b$  with  $i = 1, 2, \dots, q$  and the remaining  $n - q$  eigenvalues satisfy  $\lambda_i \leq b$  with  $i = m + 1, m + 2, \dots, n$ . Clearly, the integer  $q$  can be chosen from 0 to  $n$ . Accordingly, denote  $r_* := \text{rank}(\widetilde{\mathbf{X}})$  which includes the rank-deficient case,  $\mathcal{N}_{\widetilde{\mathbf{X}}}^b$  can be upper bounded by the Riemann sum as follows.

**Harmonic decay**  $\lambda_i(\widetilde{\mathbf{X}}) \propto n/i$  for  $i \in \{1, 2, \dots, r_*\}$  and  $\lambda_i(\widetilde{\mathbf{X}}) = 0$  for  $i \in \{r_* + 1, \dots, n\}$

$$\begin{aligned} \frac{1}{d} \mathcal{N}_{\widetilde{\mathbf{X}}}^b &= \frac{1}{d} \sum_{i=1}^{r_*} \frac{n/i}{(b + n/i)^2} = \frac{1}{d} \sum_{i=1}^q \frac{n/i}{(b + n/i)^2} + \frac{1}{d} \sum_{i=q+1}^{r_*} \frac{n/i}{(b + n/i)^2} \\ &\leq \frac{1}{nd} \int_1^{q+1} \frac{t}{(1 + \frac{bt}{n})^2} dt + \frac{1}{nd} \int_{q+1}^{r_*+1} \frac{t}{(1 + \frac{bt}{n})^2} dt \\ &= \frac{n}{b^2 d} \int_{\frac{b}{n}}^{\frac{(r_*+1)b}{n}} \frac{u}{(1+u)^2} du \text{ with the change of variable } u = tb/n \\ &= \frac{n}{b^2 d} \left[ \ln \frac{n + (r_* + 1)b}{n + b} + \frac{n}{n + b + r_* b} - \frac{n}{n + b} \right] \\ &\leq \frac{n}{b^2 d} \ln \frac{n + (r_* + 1)b}{n + b} = \mathcal{O}\left(\frac{n}{b^2 d}\right). \end{aligned}$$

**Polynomial decay:**  $\lambda_i(\widetilde{\mathbf{X}}) \propto ni^{-2a}$  with  $a > 1/2$  for  $i \in \{1, 2, \dots, r_*\}$  and  $\lambda_i(\widetilde{\mathbf{X}}) = 0$  for  $i \in \{r_* + 1, \dots, n\}$ . Hence, we actually aim to bound

$$\begin{aligned} \frac{1}{d} \mathcal{N}_{\widetilde{\mathbf{X}}}^b &= \frac{1}{d} \sum_{i=1}^{r_*} \frac{ni^{-2a}}{(b + ni^{-2a})^2} = \frac{1}{d} \sum_{i=1}^q \frac{ni^{-2a}}{(b + ni^{-2a})^2} + \frac{1}{d} \sum_{i=q+1}^{r_*+1} \frac{ni^{-2a}}{(b + ni^{-2a})^2} \\ &\leq \frac{1}{nd} \int_1^{r_*+1} \frac{t^{2a}}{(1 + \frac{t^{2a}b}{n})^2} dt \\ &= \frac{1}{2abd} \left(\frac{n}{b}\right)^{\frac{1}{2a}} \int_{b/n}^{(r_*+1)^{2a}b/n} \frac{u^{\frac{1}{2a}}}{(1+u)^2} du \text{ with the change of variable } u = t^{2a}b/n \\ &\leq \tilde{C} \frac{1}{2abd} \left(\frac{n}{b}\right)^{\frac{1}{2a}} \quad \text{since the integral is finite due to } 2a > 1 \end{aligned}$$

**Exponential decay:**  $\lambda_i(\widetilde{\mathbf{X}}) \propto ne^{-ai}$  with  $a > 0$  for  $i \in \{1, 2, \dots, r_*\}$  and  $\lambda_i(\widetilde{\mathbf{X}}) = 0$  for  $i \in \{r_* + 1, \dots, n\}$ .

We aim to bound the sum as

$$\begin{aligned}
\frac{1}{d} \mathcal{N}_{\bar{\mathbf{X}}}^b &= \frac{1}{d} \sum_{i=1}^{r_*} \frac{ne^{-ai}}{(b + ne^{-ai})^2} = \frac{1}{d} \sum_{i=1}^q \frac{ne^{-ai}}{(b + ne^{-ai})^2} + \frac{1}{d} \sum_{i=q+1}^{r_*} \frac{ne^{-ai}}{(b + ne^{-ai})^2} \\
&\leq \frac{1}{d} \int_1^{r_*+1} \frac{ne^{-at}}{(b + ne^{-at})^2} dt \\
&= \frac{1}{ad} \int_{ne^{-a(r_*+1)}}^{ne^{-a}} \frac{1}{(b + u)^2} du \text{ with the change of variable } u = ne^{-at} \\
&= \frac{1}{ad} \left( \frac{1}{b + ne^{-a(r_*+1)}} - \frac{1}{b + ne^{-a}} \right).
\end{aligned}$$

Note that, the monotonicity of  $\mathcal{N}_{\bar{\mathbf{X}}}^b$  (also  $\mathbf{V}_1$ ) with respect to  $n$  is relatively clear for *harmonic decay* and *polynomial decay* but is unclear in the case of *exponential decay*. Here we study the monotonicity in the *exponential decay*. Denote the function  $G(n) := \left( \frac{1}{b + ne^{-a(r_*+1)}} - \frac{1}{b + ne^{-a}} \right)$  with  $b := n\lambda + \gamma$ , taking  $\lambda := \bar{c}n^{-\vartheta}$ , its derivation is

$$G'(n) = \frac{-\bar{c}(1-\vartheta)n^{-\vartheta} - e^{-a(r_*+1)}}{[cn^{1-\vartheta} + \gamma + ne^{-a(r_*+1)}]^2} + \frac{\bar{c}(1-\vartheta)n^{-\vartheta} + e^{-a}}{[cn^{1-\vartheta} + \gamma + ne^{-a}]^2}, \quad (\text{F.1})$$

which can be rewritten as

$$G'(n) = \frac{\bar{c}(1-\vartheta)n^{-\vartheta} + e^{-a}}{[cn^{1-\vartheta} + \gamma + ne^{-a(r_*+1)}]^2} \left( \underbrace{\frac{[\bar{c}n^{1-\vartheta} + \gamma + ne^{-a(r_*+1)}]^2}{[\bar{c}n^{1-\vartheta} + \gamma + ne^{-a}]^2}}_{\triangleq H_1(n)} - \underbrace{\frac{\bar{c}(1-\vartheta)n^{-\vartheta} + e^{-a(r_*+1)}}{\bar{c}(1-\vartheta)n^{-\vartheta} + e^{-a}}}_{\triangleq H_2(n)} \right).$$

It can be found that both  $H_1(n)$  and  $H_2(n)$  are decreasing functions with  $n$ . More specifically, their maximum and minimum can be achieved with

$$\max_n H_1(n) = H_1(1) = \left( \frac{\bar{c} + \gamma + e^{-a(r_*+1)}}{\bar{c} + \gamma + e^{-a}} \right)^2, \quad \min_n H_1(n) = \lim_{n \rightarrow \infty} H_1(n) = \left( \frac{e^{-a(r_*+1)}}{e^{-a}} \right)^2,$$

and

$$\max_n H_2(n) = H_2(1) = \frac{\bar{c}(1-\vartheta) + e^{-a(r_*+1)}}{\bar{c}(1-\vartheta) + e^{-a}}, \quad \min_n H_2(n) = \lim_{n \rightarrow \infty} H_2(n) = \frac{e^{-a(r_*+1)}}{e^{-a}}.$$

Accordingly, if  $H_1(1) < H_2(1)$ , we obtain a decreasing function  $G(n)$  of  $n$ , which implies that  $\mathcal{N}_{\bar{\mathbf{X}}}^b$  will decrease with  $n$ . Here the condition  $H_1(1) < H_2(1)$  indicates

$$\left( \frac{\bar{c} + \gamma + e^{-a(r_*+1)}}{\bar{c} + \gamma + e^{-a}} \right)^2 \leq \frac{\bar{c}(1-\vartheta) + e^{-a(r_*+1)}}{\bar{c}(1-\vartheta) + e^{-a}},$$

which is equivalent to

$$(\vartheta\bar{c} + \gamma)^2 \leq [e^{-a} + (1-\vartheta)\bar{c}] [e^{-a(r_*+1)} + (1-\vartheta)\bar{c}]. \quad (\text{F.2})$$

Accordingly, if the above inequality holds,  $\mathcal{N}_{\bar{\mathbf{X}}}^b$  will decrease with  $n$ . In Section G.2, we will experimentally check whether this condition holds or not.

## F.2 $n > d$ case and the large $n$ limit

In this section, we consider the  $n > d$  case, and further study the trend of  $\mathbf{V}_1$  as  $n \rightarrow \infty$ . Note that, in this case,  $\mathbf{X}\mathbf{X}^T/d$  has at most  $r_* \leq d$  non-zero eigenvalues. Accordingly, the Riemann sum is counted to  $r_*$  instead of  $n$ . Similar to the above description, we also consider the following three eigenvalue decays.

**Harmonic decay**  $\lambda_i(\widetilde{\mathbf{X}}) \propto n/i$ ,  $i \in \{1, 2, \dots, d\}$

$$\begin{aligned} \frac{1}{d} \mathcal{N}_{\widetilde{\mathbf{X}}}^b &= \frac{1}{d} \sum_{i=1}^{r_*} \frac{n/i}{(b+n/i)^2} = \frac{1}{d} \sum_{i=1}^q \frac{n/i}{(b+n/i)^2} + \frac{1}{d} \sum_{i=q+1}^{r_*} \frac{n/i}{(b+n/i)^2} \\ &\leq \frac{n}{b^2 d} \int_{\frac{b}{n}}^{\frac{(r_*+1)b}{n}} \frac{u}{(1+u)^2} du \\ &= \frac{n}{b^2 d} \left[ \ln \frac{n+(r_*+1)b}{n+b} + \frac{n}{n+b+r_*b} - \frac{n}{n+b} \right]. \end{aligned}$$

In particular, taking the limit of  $n \rightarrow \infty$ , we have

$$\begin{aligned} \lim_{n \rightarrow \infty} \frac{1}{d} \mathcal{N}_{\widetilde{\mathbf{X}}}^b &= \lim_{n \rightarrow \infty} \frac{n}{b^2 d} \left[ \ln \frac{n+(r_*+1)b}{n+b} + \frac{n}{n+b+r_*b} - \frac{n}{n+b} \right] \\ &= \lim_{n \rightarrow \infty} \frac{n}{b^2 d} \ln \frac{n+(r_*+1)b}{n+b} + \lim_{n \rightarrow \infty} \frac{n}{b^2 d} \left( \frac{n}{n+b+r_*b} - \frac{n}{n+b} \right) \\ &= \frac{r_*}{d} \left( \lim_{n \rightarrow \infty} \frac{1}{b} \frac{n}{n+b} - \lim_{n \rightarrow \infty} \frac{n^2}{b(n+b+r_*)(n+b)} \right) \\ &\leq \lim_{n \rightarrow \infty} \frac{1}{b} \frac{n}{n+b} - \lim_{n \rightarrow \infty} \frac{n^2}{b(n+b+r_*)(n+b)} \\ &= 0. \end{aligned}$$

Accordingly, by the squeeze theorem, we can conclude, given  $d$ ,  $\mathcal{N}_{\widetilde{\mathbf{X}}}^b$  tends to zero when  $n \rightarrow \infty$ .

**Polynomial decay:**  $\lambda_i(\widetilde{\mathbf{X}}) \propto ni^{-2a}$  with  $a > 1/2$ ,  $i \in \{1, 2, \dots, d\}$

$$\begin{aligned} \frac{1}{d} \mathcal{N}_{\widetilde{\mathbf{X}}}^b &= \frac{1}{d} \sum_{i=1}^{r_*} \frac{ni^{-2a}}{(b+ni^{-2a})^2} \leq \frac{1}{2abd} \left( \frac{n}{b} \right)^{\frac{1}{2a}} \int_{b/n}^{(r_*+1)^{2a}b/n} \frac{u^{\frac{1}{2a}}}{(1+u)^2} du \\ &\leq \frac{1}{2abd} \left( \frac{n}{b} \right)^{\frac{1}{2a}} \int_0^\infty \frac{u^{\frac{1}{2a}}}{(1+u)^2} du \\ &\leq \widetilde{C} \frac{1}{2abd} \left( \frac{n}{b} \right)^{\frac{1}{2a}} \quad \text{since the integral is finite due to } 2a > 1 \end{aligned}$$

Since the integral  $\int \frac{u^{\frac{1}{2a}}}{(1+u)^2} du$  can behave rather differently for different choices of  $a$ , here we take  $a = 1$  as an example. Taking the limit of  $n \rightarrow \infty$ , we have

$$\begin{aligned} \lim_{n \rightarrow \infty} \frac{1}{d} \mathcal{N}_{\widetilde{\mathbf{X}}}^b &= \lim_{n \rightarrow \infty} \frac{1}{2bd} \left( \frac{n}{b} \right)^{\frac{1}{2}} \int_{b/n}^{(r_*+1)^2b/n} \frac{u^{\frac{1}{2}}}{(1+u)^2} du \\ &= \frac{1}{2bd} \lim_{n \rightarrow \infty} \left( \frac{n}{b} \right)^{\frac{1}{2}} \left( \arctan(\sqrt{u}) - \frac{\sqrt{u}}{u+1} \right) \Bigg|_{b/n}^{(r_*+1)^2b/n} \\ &= \frac{1}{2bd} \lim_{n \rightarrow \infty} \sqrt{\frac{n}{b}} \left( (r_*+1)\sqrt{b/n} - \frac{(r_*+1)\sqrt{b/n}}{(r_*+1)^2b/n} - \sqrt{b/n} + \frac{\sqrt{b/n}}{b/n+1} \right) \text{ using } \lim_{x \rightarrow 0} \frac{\arctan x}{x} = 1. \\ &= 0. \end{aligned}$$

**Exponential decay:**  $\lambda_i(\widetilde{\mathbf{X}}) \propto ne^{-ai}$  with  $a > 0, i \in \{1, 2, \dots, d\}$

$$\begin{aligned} \frac{1}{d} \mathcal{N}_{\widetilde{\mathbf{X}}}^b &= \frac{1}{d} \sum_{i=1}^{r_*} \frac{ne^{-ai}}{(b + ne^{-ai})^2} = \frac{1}{d} \sum_{i=1}^q \frac{ne^{-ai}}{(b + ne^{-ai})^2} + \frac{1}{d} \sum_{i=q+1}^{r_*} \frac{ne^{-ai}}{(b + ne^{-ai})^2} \\ &\leq \frac{1}{ad} \int_{ne^{-a(r_*+1)}}^{ne^{-a}} \frac{1}{(b + u)^2} du \\ &= \frac{1}{ad} \left( \frac{1}{b + ne^{-a(r_*+1)}} - \frac{1}{b + ne^{-a}} \right). \end{aligned}$$

Taking the limit of  $n \rightarrow \infty$ , we can directly have  $\lim_{n \rightarrow \infty} \frac{1}{d} \mathcal{N}_{\widetilde{\mathbf{X}}}^b = 0$ .

## G Additional Experiments

In this section, we present additional experiments including the following parts:

- In Section G.1, we add the *MNIST* dataset [LBBH98] to verify the eigenvalue decay equivalence, and evaluate the effect by different orders in polynomial kernel.
- In Section G.2, our model works in a polynomial kernel setting under the *polynomial decay* and *exponential decay* of  $\widetilde{\mathbf{X}}$  on the synthetic dataset.
- In Section G.3, we investigate the relationship between the position of the peak point and the regularization parameter  $\lambda$ .

### G.1 Eigenvalue decay equivalence

Apart from the *YearPredictionMSD* dataset in the main text, we add the *MNIST* dataset [LBBH98] to verify the eigenvalue decay equivalence. We also compute eigenvalues of  $\widetilde{\mathbf{X}} := \beta \mathbf{X} \mathbf{X}^\top / d + \alpha \mathbf{1} \mathbf{1}^\top$  for validation. Here the parameters  $\alpha$  depends on the covariate  $\Sigma_d$ , which can be empirically estimated by the sample covariance  $\frac{1}{n} \sum_{i=1}^n (\mathbf{x}_i - \frac{1}{n} \sum_{j=1}^n \mathbf{x}_j)(\mathbf{x}_i - \frac{1}{n} \sum_{j=1}^n \mathbf{x}_j)^\top$ .

Results on the polynomial kernel with order 3 and the Gaussian kernel are presented in Figure 6 and 7, respectively. It can be observed that, the nonlinear kernel matrix  $\mathbf{K}$  admits almost the same eigenvalue as  $\widetilde{\mathbf{X}} := \beta \mathbf{X} \mathbf{X}^\top / d + \alpha \mathbf{1} \mathbf{1}^\top$  with a constant shift  $\gamma$ , and accordingly exhibits the same eigenvalue decay with  $\widetilde{\mathbf{X}}$  and  $\mathbf{X} \mathbf{X}^\top / d$ .

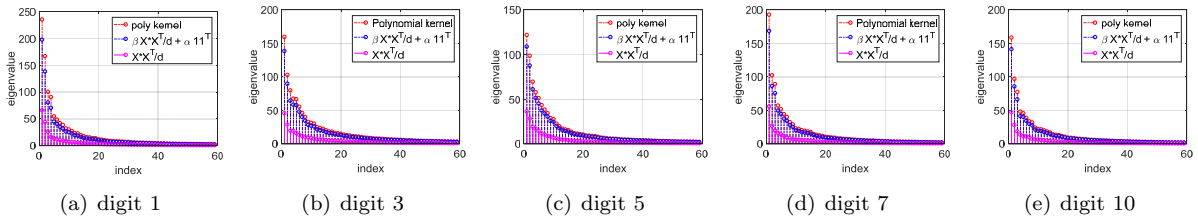


**Figure 6.** Top 60 eigenvalues of Polynomial kernel with order 3 and its linearization on the MNIST dataset. Note that the largest eigenvalue  $\lambda_1$  is not plotted for better display.

Besides, to study eigenvalue decay effected by the order in polynomial kernels, we present results of the order  $p = 5$  and  $p = 10$  in Figure 8. Experimental results show that, there is some gap between the original kernel and its linearization in higher orders. This is because, nonlinear kernel approximated by linear model here is based on Taylor expansion, which would incur in some residual errors as higher order in polynomial kernels brings in stronger non-linearity.

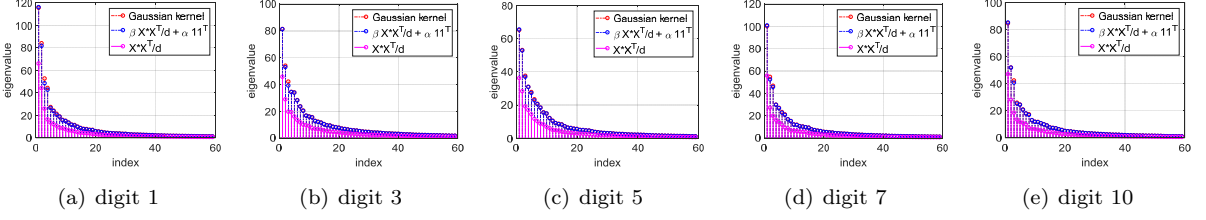


**Figure 7.** Top 60 eigenvalues of Gaussian kernel and its linearization on the MNIST dataset. Note that the largest eigenvalue  $\lambda_1$  is not plotted for better display.

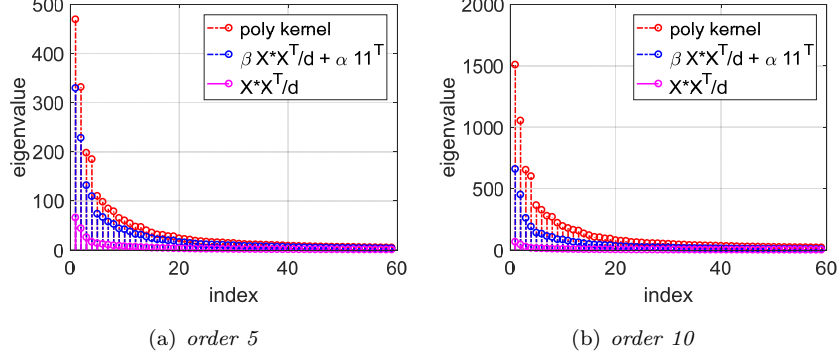


**Figure 8.** Top 60 eigenvalues of polynomial kernel matrices and their linearizations on the MNIST dataset (digit 1). Note that the largest eigenvalue  $\lambda_1$  is not plotted for better display.

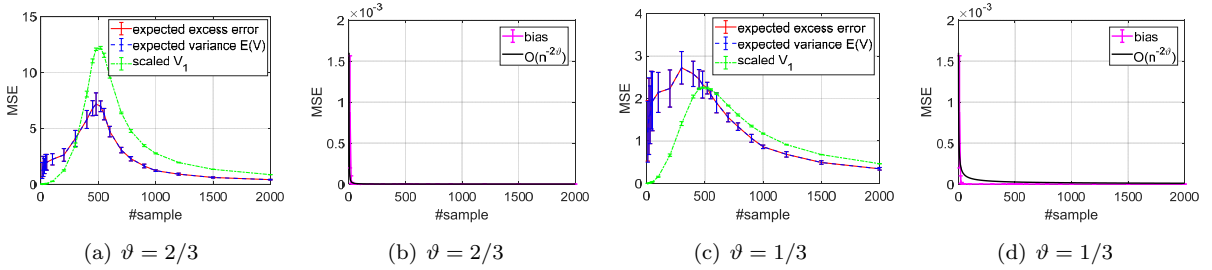


**Figure 9.** Polynomial decay of  $\widetilde{\mathbf{X}}$  in the polynomial kernel case: MSE of the expected excess risk, the variance in Eq. (3.6), our derived  $V_1$ , the bias in Eq. (3.5), and our derived convergence rate  $\mathcal{O}(n^{-2\vartheta r})$  with  $r = 1$  in Theorem 2 under different  $\vartheta$ .

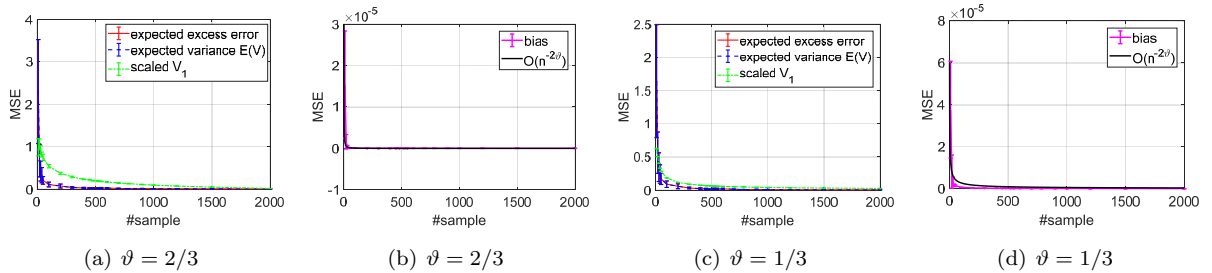


**Figure 10.** Exponential decay of  $\widetilde{\mathbf{X}}$  in the polynomial kernel case: MSE of the expected excess risk, the variance in Eq. (3.6), our derived  $V_1$ , the bias in Eq. (3.5), and our derived convergence rate  $\mathcal{O}(n^{-2\vartheta r})$  with  $r = 1$  in Theorem 2 under different  $\vartheta$ .

## G.2 Results on the synthetic dataset

Here we evaluate our model with the polynomial kernel on the synthetic dataset under the polynomial/exponential decay of  $\widetilde{\mathbf{X}}_d$ . The data generation process follows with our experiments part in the main text such that  $\widetilde{\mathbf{X}}$  admits the polynomial/exponential decay.

Results on the *polynomial decay* and the *exponential decay* are shown in Figure 9 and Figure 10, respectively. We find that, the bias achieves the certain  $\mathcal{O}(n^{-2\vartheta r})$  convergence rate on both decays; while the variance shows different configurations on these two decays. To be specific, the tend of  $V_1$  on the *polynomial decay* is unimodal, and thus the risk curve is bell-shaped. However, in Figure 10,  $V_1$  on the *exponential decay* monotonically decreases with  $n$  even if we set  $\bar{c}$  to  $10^{-5}$ ,  $10^{-8}$  for a small regularization scheme.

Here we attempt to explain this phenomenon. In our setting,  $\gamma$  is set to zero. The condition in Eq. (F.2) can be reformulated as

$$(2\vartheta - 1)\bar{c} \leq e^{-a}(1 - \vartheta).$$

Clearly, if we choose  $0 < \vartheta < 1/2$ , the condition in Eq. (F.2) always holds. Hence,  $V_1$  will monotonically decreases with  $n$ . If  $1/2 < \vartheta < 1$ , we examine our result with  $a = 1$  and  $\vartheta = 2/3$ . We conclude that the used  $\bar{c} = 0.01 < e^{-1}$ , so the tend of  $V_1$  is monotonically decreasing with  $n$ .

## G.3 Relationship between the position of the peak point and the regularization

Hastie et al. [HMRT19] demonstrate that the regularization parameter  $\lambda$  (independent of  $n$ ) does not effect the position of the peak point, only changes its magnitude. Here we conduct our experiments two settings: one is to use an small  $\bar{c} := 10^{-5}$  such that  $\lambda := \bar{c}n^{-\vartheta}$  is small but depends on  $n$ ; the other is to directly set  $\lambda$  to a specific value independent of  $n$ . Specifically, we set  $\gamma = 0$  to disentangle the *implicit regularization* effect on the final result.

### G.3.1 A small $\lambda$ that depends on $n$

Here we test our model with the polynomial/Gaussian kernel and the *harmonic decay* on the synthetic dataset. In this experiment,  $\bar{c} := 10^{-5}$  allows for a small regularization parameter  $\lambda := \bar{c}n^{-\vartheta}$ . Results on the polynomial kernel (Figure 11) and the Gaussian kernel (Figure 12) demonstrate that, a small  $\lambda$  depending on  $n$  does not effect the position of the peak point, but largely effects its value. Specifically, our derived bounds perfectly fit the variance and bias, which illustrates that our upper bounds are tight and accurate.

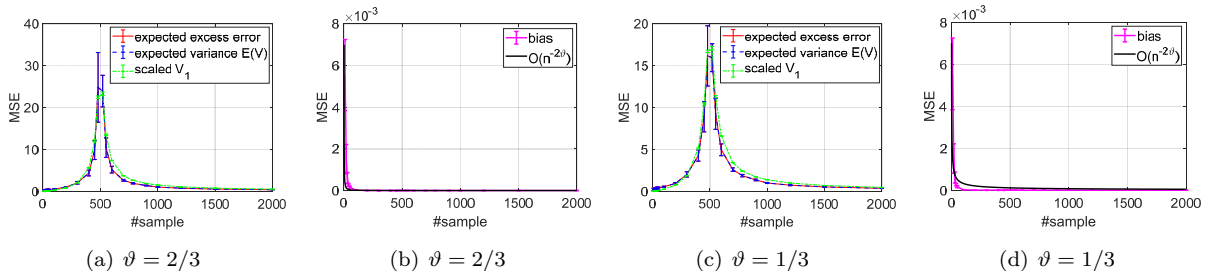


**Figure 11.**  $\bar{c} = 10^{-5}$ : Harmonic decay of  $\widetilde{\mathbf{X}}$  in the polynomial kernel case: MSE of the expected excess risk, the variance in Eq. (3.6), our derived  $V_1$ , the bias in Eq. (3.5), and our derived convergence rate  $\mathcal{O}(n^{-2\vartheta r})$  with  $r = 1$  in Theorem 2 under different  $\vartheta$ .

### G.3.2 A small $\lambda$ that is independent of $n$

Here we choose the regularization parameter  $\lambda$  independent of  $n$  to observe the position of the peak point on the subset of the *YearPredictionMSD* dataset. In our setting, the imposed  $\lambda$  is the only regularization scheme as  $\gamma = 0$ . More importantly,  $\lambda$  is independent of  $n$ . Figure 13 shows that, when  $\lambda$  is independent of  $n$ , the position of the peak point almost stays unchanged, around  $n := d = 90$ . But along with a large  $\lambda$ , the magnitude of the peak decreases until disappears. Accordingly, our experiments recover the result of [HMRT19].



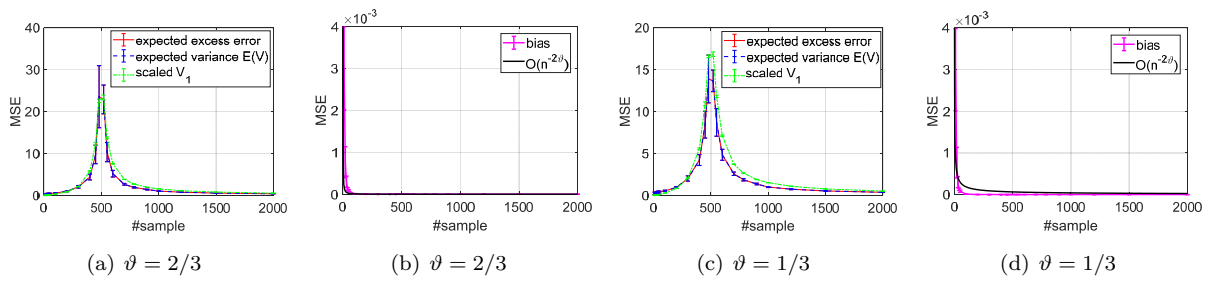


**Figure 12.**  $\bar{c} = 10^{-5}$ : Harmonic decay of  $\widetilde{\mathbf{X}}$  in the Gaussian kernel case. The legend is the same as Figure 11.

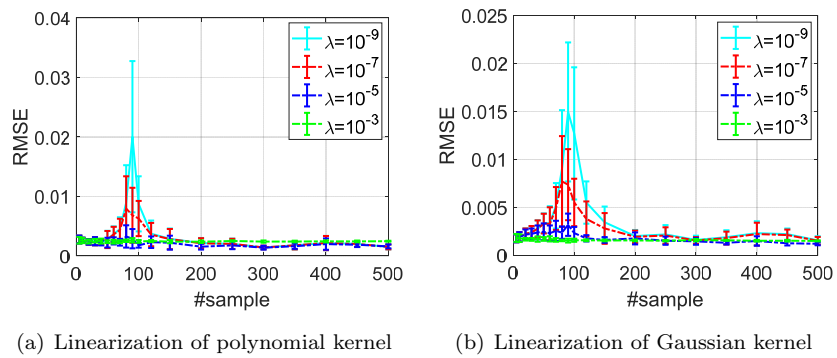


**Figure 13:** RMSE on the subset of the *YearPredictionMSD* dataset.